Ecole Polytechnique Fédérale de Lausanne (EPFL)

Master Thesis

# Evaluation of the potential of the solar thermal in district heating networks in Switzerland

August 23, 2021

*Author:*
Maximilien Clappier

*Supervisors:*
Dr. Jérôme Kämpf, kaemco
Prof. Paolo Ricci, EPFL

# Acknowledgements

*I* thank Jérôme Kämpf, my supervisor during my thesis at kaemco for the time he gave me. His advice has always been useful and helped me to move forward. I thank Paolo Ricci who accepted to be my supervisor even though the topic of the thesis was not in his domain. I thank Dewaraz, and Giona Galizia from RWB. They brought me their experience on the simulation of district heating networks. I wanted to thank the partners Altis, Planair, municipality of Yverdon, who provided me the necessary information in order to build the case studies for the simulation. I also thank my kaemco colleagues coming from Belgium who made me re-discover Switzerland. I thank the entire CREM that kindly gave me a seat in their office. Finally, I thank my friends and family for all the support they provided me during this thesis and my studies.

# Abstract

*A*n evaluation of the potential of the solar thermal in district heating networks in Switzerland has been performed. Simulations have been carried out in order to compare different scenarios. For this purpose, the open-source simulation tool CitySim has been used and developed to study district heating networks.

The CitySim computational framework was already capable of simulating detailed urban physics connected to complex topologies of district heating networks, such as looped networks with multiple heating stations. However, it was not yet validated on complex real case studies. Before doing the validation, new implementations have been carried out. As an example, CitySim needed to define some rules in order to be able to simulate, in a more accurate way, networks with multiple heating stations.

Taking into account the new implementations, two different case studies were considered in order to perform the validation, the branched network of Broc which was already used in a former validation, and the looped one of Verbier. These validations were satisfying but showed the necessity of having complete databases on each network as well as the methods used by the operators in order to monitor their district heating network.

In the optic of evaluating the solar potential in district heating, a study on the low enthalpy network of Yverdon has been driven. At first, the CitySim tool has been modified in order to be able to simulate low-temperature district heating network with the implementation of new connecting elements with the network.

In the end, different connecting scenarios have been evaluated, in which some of them were considering the injection of solar thermal in the network. CitySim allowed through these different scenarios to evaluate the best candidate based on the thermal losses and the electricity consumption in the network.

# Summary


**1 Introduction** **1**
- 1.1 General context . . . 1
- 1.2 State of the art . . . 3
- 1.3 Problematic . . . 3
- 1.4 Thesis content . . . 4

**2 Original status of CitySim** **5**
- 2.1 District heating networks . . . 5
- 2.2 Buildings . . . 6
- 2.3 Network . . . 8
  - 2.3.1 Hydraulic convergence . . . 8
  - 2.3.2 Thermal convergence . . . 9
- 2.4 Heating stations . . . 10
- 2.5 Overall control . . . 10

**3 New implementations in CitySim** **13**
- 3.1 Implementation of singular pressure losses . . . 13
- 3.2 District heating networks with multiple heating stations . . . 15
  - 3.2.1 Measure Control Regulation . . . 15
  - 3.2.2 Slave heating stations . . . 17
  - 3.2.3 Overall control . . . 19

**4 Validation of the CitySim tool** **21**
- 4.1 Results of CitySim simulation on case studies . . . 22
  - 4.1.1 Broc: Branched network with a single heating station . . . 22
  - 4.1.2 Verbier: Looped network with multiple heating stations . . . 26

**5 Case study of Yverdon: Application to a low enthalpy district heating network** **37**
- 5.1 Introduction . . . 37
  - 5.1.1 Historical details about district heating networks . . . 37
  - 5.1.2 Presentation of the case study . . . 38
- 5.2 Implementation of the connecting elements . . . 39
  - 5.2.1 The Substation Heat Pump . . . 40
  - 5.2.2 The substation 2-stages Heat Pump . . . 41
- 5.3 Validation of the CitySim tool on the case study of Yverdon . . . 43
  - 5.3.1 Hypothesis and benchmark . . . 44
  - 5.3.2 Results on the 2021 scenario . . . 45
- 5.4 Scenarios between the different connecting elements . . . 49
  - 5.4.1 Comparison between the 1-stage and 2-stages heat pumps . . . 49

5.4.2 Comparison between centralised and decentralised heat pumps . . . . . . . . . 51
5.5 Solar district heating . . . . . . . . . . . . . . . . . . . . . . . . . . . . . . . . . . . . . 54
5.5.1 Comparison between centralised and decentralised injection . . . . . . . . . . . 54
5.5.2 Sizing of the storage heat tank . . . . . . . . . . . . . . . . . . . . . . . . . . . 55
5.5.3 Comparison between different injection temperature . . . . . . . . . . . . . . . 56

**6 Conclusion** **58**

# Figures


1.1 *Breakdown of Switzerland's total greenhouse gas emissions into sectors in accordance with the CO2 Ordinance in 1990 and 2019.[4]* . . . . . 2

2.1 *Simplified schematics of a district heating network designed by Pierre Cognet.* . . . . . 6
2.2 *Decomposition of the network in Fig.2.1 into several loops.* . . . . . 9

3.1 *Table displaying the K factor for different ratio of mass flows in the connected pipes having the same radius R. [18]* . . . . . 14
3.2 *Schematics of the hydraulic model of the slave heating station. When the thermal station supply the network, the three-way valves connect the heat exchanger to the pump, leaving the valve unused. In that case, the flow goes from return to supply and the three-way valves help the pump to control the mass flow. When the thermal station is shut down, the three-way valves connect the heat exchanger to the valve that prevent the flow to go from supply to return.* . . . . . 17

4.1 *Topographic map of Broc (left) and the QGIS visualisation of the district heating network with consumers in grey and the heating station in green in 2019 (right) [14].* 22
4.2 *The comparison between the CitySim simulation and the measurement at the heating station for the mass flow, the power delivered, the entering and exiting temperatures (middle), and the temperature difference starting on the 1st of October 2018 at midnight.* . . . . . 24
4.3 *Distribution of the absolute error between the CitySim simulation and the measurement on the mass flow, the power delivered and the exiting and entering temperatures at the heating station starting on the 1st of October 2018 at midnight.* . . . . . 25
4.4 *Map of the district heating network of Verbier in 2019.* . . . . . 26
4.5 *Table containing information related to the pipes in the PostgreSQL database on the network of Verbier in 2019.* . . . . . 27
4.6 *Table containing information related to the nodes in the PostgreSQL database for the network of Verbier in 2019.* . . . . . 27
4.7 *The comparison between the CitySim simulation and the measurement at the Trois Rocs thermal station for the mass flow (left), the entering temperature (middle) and temperature difference between the entering and exiting temperature (right).* . . . . . 29
4.8 *Distribution of the absolute errors between the CitySim simulation and the measurement on the mass flow (left) and the entering temperature (right) at the Trois Rocs thermal station, with the 95% confidence interval. Considering the period going from the 1st of January to the 28th of May 2019.* . . . . . 29
4.9 *The evolution and the distribution of the error of the thermal power delivered at the Trois Rocs thermal station.* . . . . . 30
4.10 *Comparison between the results of CitySim and the measured data at the substation 860.* . . . . . 31

4.11 *Distribution of the absolute errors between the CitySim simulation and the measurement on the overall buildings with the 95% confidence interval for the benchmarks of the substation and the errors on the target temperature of $\Delta T = 30°C$ at every substation. Considering the period going from the 1st of January to the 28th of May 2019.* . . . 32
4.12 *Comparison between the results of CitySim with the measured data at the substation 2704.* . . . 33
4.13 *The comparison between the measured and simulated thermal losses of the network of Verbier along the total power provided by the heating station, the total power consumed by the buildings and the estimated ground temperature at a depth of 1m.* . . . 34
4.14 *Evolution of the thermal power (left) and exiting temperatures (right) for the two heating stations, with the hour 1 corresponding to the 1st of January 2019.* . . . 35
4.15 *GIF of the evolution of the supply temperature and the mass flow in the network of Verbier following the MCR implemented in CitySim.* . . . 35

5.1 *QGIS visualisation of the district heating network of Yverdon. The different colors represent the different extensions that are planned while the numbers appearing close to the DHN correspond to the nominal diameter of the pipes.* . . . 38
5.2 *Partial content of the table pipe in the PostgreSQL database describing the network of Yverdon.* . . . 39
5.3 *The schematics of a heat pump.* . . . 40
5.4 *The schematics of the two stages heat pump implemented in CitySim.* . . . 41
5.5 *The characteristic curve of the pump at the heat exchanger STAP of the STEP. [24]* 44
5.6 *The measured exiting temperature of the STAP with a data completion from August 2021 to the end.* . . . 45
5.7 *Time evolution of the temperatures and mass flows through the actual network of Yverdon (right supply, left return). The temperatures are given at the nodes while the mass flows are given at the pipes.* . . . 46
5.8 *Time evolution of the regular together with the singular pressure differences through the actual network of Yverdon.* . . . 46
5.9 *Validation of the implementation of the SubstationHeatPump on the Marive building.* 47
5.10 *Time evolution of the thermal losses in the actual network of Yverdon (right supply, left return).* . . . 48
5.11 *Comparison between the electric consumption at the Marive substation (left) and at the pump of the heating station (right) with 1-stage and 2-stages heat pumps.* . . . 50
5.12 *Comparison between the total electric consumption in the actual network of Yverdon with 1-stage and 2-stages heat pumps.* . . . 50
5.13 *Annual KPIs for the different forecast extension of the network* . . . 51
5.15 *Comparison between the decentralised and centralised heat pump cases on the electricity consumption (left) and thermal losses (right) on the low temperature DHN.* . . . 52
5.14 *QGIS visualisation of the centralised heat pump and the decentralised heat pump scenarios. The centralised heat pump is represented with the red point and supplies all the buildings on the map.* . . . 52
5.16 *Time evolution of the pressure differences through the forecast centralised network of 2026 in Yverdon.* . . . 53
5.17 *Evolution of the temperature inside the storage tank at the heating station for various heat capacity in J/K for the first year of operation.* . . . 55

# Tables

5.1 *Hypothesis considered for the simulation on the DHN of Yverdon. [24]* . . . . . . . . . 44
5.2 *The hourly means of the thermal losses and total electric consumption in the network on the 11th of January 2021. The relative thermal losses with respect to the thermal power delivered by the wastewater treatment plant.* . . . . . . . . . . . . . . . . . . . . . 49
5.3 *Comparison of the yearly KPIs between the centralised and decentralised heat pump.* 53
5.4 *The comparison of the total thermal power provided by the heating station, total electricity consumption and total thermal loss between the centralised and decentralised solar injection over one year.* . . . . . . . . . . . . . . . . . . . . . . . . . . . . . . . . . 55
5.5 *The energy delivered by the WWTP during the year 2021 considering different sizes of storage.* . . . . . . . . . . . . . . . . . . . . . . . . . . . . . . . . . . . . . . . . . 56
5.6 *The energy delivered by the WWTP along the KPIs considering different temperatures of injection.* . . . . . . . . . . . . . . . . . . . . . . . . . . . . . . . . . . . . . . 57

# CHAPTER 1

# INTRODUCTION

## 1.1 General context

Since the beginning of the twentieth century and the industrial revolution, the energy demand has significantly increased due to the population growth and the improvement of the quality of life. Nowadays, energy is present in every sectors of our society. Although it used in a wide variety of forms, it is almost entirely produced by the combustion of fossil fuels such as coal, oil or gas. This intensive use of these resources is the origin of many issues.

First of all, fossil fuels are not renewable. They originate from the sequestration of biomass(forests and other organic sediments such as ocean plankton) that have been buried and pressurized for millions of years in the ground. If our energy consumption continues to rise, oil and gas stocks are expected to be depleted in the next few decades, while coal reserves could last another century [1]. Being not prepared for these events could have dramatic issues and paralysed every sector going from transport to health care. In addition, the combustion of fossil fuels generates exhaust gases which are responsible for air pollution and climate change. According to the World Health Organization (WHO), a fifth of the current death could be attributed to the air pollution [2]. The effect of climate could be just as devastating as the first two as sea level rising and major heat waves will create huge migration flows around the world. For all these reasons, it is therefore of primordial importance to move away from this dependence and represents one of the major challenges that our modern societies have to face in the next decades.

In this context, Switzerland has established a strategy in order to reduce the environmental impact of the Swiss population. One of the main commitments is to reduce by half the greenhouse gas emissions which are responsible for climate change by 2030 with respect to 1990 and to reach zero net greenhouse gas emissions in the horizon of 2050. In order to achieve these objectives, the most polluting sectors have been identified [3]. Following, the study from the Federal Office for the Environment (FOEN) published in 2019, the household sector was the third biggest contributor of greenhouse gas emissions after the sector of transport and industry. The Fig. 1.1 shows that 16.6% of the GHG emissions can be attributed to the household. These emissions are mainly coming from the exhaust gases of the combustion of fossil fuels. In between 1990 and 2019, the household sector has experienced the biggest decrease in GHG emissions with 25% of reduction. Nevertheless, this sector still emits approximately 8 millions of tons of equivalent $CO_2$ per year nowadays. Improvements are still possible in this sector since 67.2% of Swiss buildings are burning fossil fuels for their heating [6]. The control of these emissions follows two main strategies. On the first side, demand has to be reduced, for example, improving the insulation of buildings or increasing the efficiency of energy conversion systems. On the second side, by using cleaner technologies such as solar thermal or heat pumps.

In this context, the district heating networks are fundamental and will play an important role

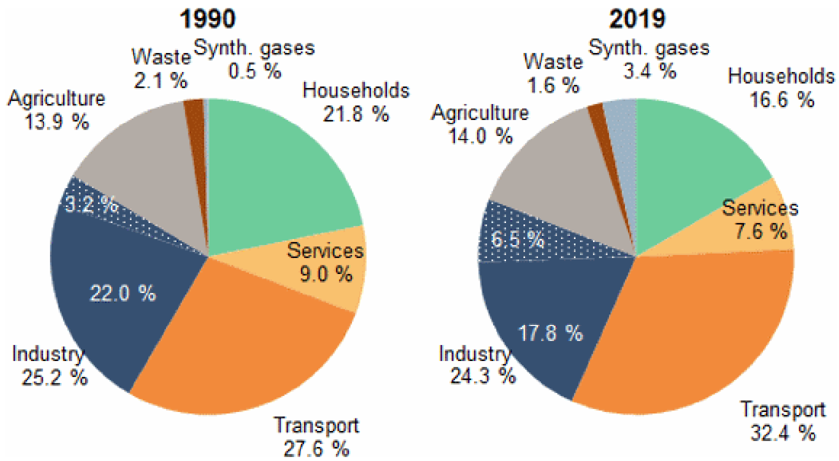


Figure 1.1: *Breakdown of Switzerland's total greenhouse gas emissions into sectors in accordance with the CO2 Ordinance in 1990 and 2019.[4]*

in the following years [5]. First of all, it allows to heat the buildings in a more efficient way since the heat production is centralised and industrial energy conversion systems have better efficiencies than their domestic counterparts. Secondly, the exhaust gases treatment is more straightforward since they are produced only in one location. Thirdly, the district heating networks enabled shared seasonal storage and electrification of heat production, the integration of renewable energies that represent an alternative to the fossil fuels. [8] For these purposes, the FOEN encourages operators to develop this technology by offering subsidies and funding projects in Switzerland [9].

The project named SolCAD to which this thesis is linked to is, for example, partially funded by the FOEN and is part of the 2050 energy strategy. SolCAD stands for "Chauffage à Distance solaire" in french which can be translated into "solar district heating networks" in english. The overall goal of this project is to promote the integration of solar thermal in Switzerland through district heating and more specifically to achieve the following objectives:

- Extend the evaluation of the potential of solar thermal energy coupled with heat storage in district heating networks in Switzerland, while considering the technological and socio-economical constraints.
- Validate and optimize the energetic and economic performances of solar district heating networks in Switzerland, including different combination of technologies, such as solar thermal with other renewable energy sources, heat pump and storage.
- Analyse the success and limiting factors for the integration of solar thermal in DHN using a DHN archetype.

The stakeholders that are taking part to this project are presented below:

- CREM is a research center located in Martigny specialised in the domain of energy sustainability in urban areas.
- HEIG-VD is the school of engineering and management in Canton de Vaud.
- kaemco is a spin-off company of the Solar Energy and Building Physics Laboratory (LESO-PB) of EPFL. kaemco developed the computational framework named CitySim that simulates district heating networks and buildings heat demand. It provides consulting for urban energy systems. I participated to the SolCAD project in this context.

- Planair is a consulting engineering firm for sustainable development

The work performed in this thesis in the project was to further develop and use the CitySim tool in order to simulate low temperature district heating networks and the integration of solar thermal energy in these systems. Thanks to this software, it has been possible to study multiple scenarios and forecast extensions providing decision support to urban energy planners as well as promoting the development of district heating networks of the new generation to municipalities and politics.

## 1.2 State of the art

The current literature has been investigated in order to carry out this thesis.

The subject of district heating network is well documented but most of the literature found does not simulate or consider the district heating as a whole. CitySim combines the building model, the solar thermal production and storage together with district heating networks. Moreover, simulations on low temperature district heating networks are not easily found in the literature.

The paper [11] aims to simulate low temperature district heating network by using TRNSYS and Dymola.They study the district heating networks accounting for the solar thermal injection and PV implementation. Nevertheless, they consider very simplified branched networks and the solar feed-in is only centralised.

Concerning the article [12], it focuses on the modeling, control, and optimization of a low-temperature district heating network, presenting a case study with a high share of waste heat from high-performance computers. The article goes into more details in the explanation of their model. Once again, they did not have the possibility to integrate looped network or decentralised injection.

In the literature [10], the building of a model with multiple heating station is discussed together with an optimisation on the operating costs of the district heating networks considering the thermal inertia of the buildings. The goal was to optimize the operating costs by considering different regulation mode in order to satisfy the demand of the consumers of the network. They developed two model based on quality regulation mode and quantity regulation mode. The quality regulation mode considers that the the mass flow is kept constant and the supply temperature should adapt for the consumers as it is performed CitySim while the other one is the opposite. The implementation of the model is well detailed but they do not define rules in order to control the different heating stations together.

## 1.3 Problematic

Through the years, district heating networks tend to supply more consumers and be more robust for the users. They have evolved from simple tree-based shapes with one heating station to looped networks with multiple heating stations. These systems give more degrees of freedom which increases their complexity. A lot of models have been developed to simulate district heating networks and thus help the operators in the development of their facility. They allow to improve significantly the efficiency and the robustness of this technology. As a result, today, the tools as CitySim have become essential for district heating networks. Thanks to them, optimisations can be performed and predictions on future extensions can be made.

Nevertheless, modelling the dynamics of a district heating network is a real challenge as it has to simulate many different processes governed by different timescales. The changes in pressure or mass flows in the network travel at the speed of sound while the temperature goes at the same speed of the flowing water [16]. On top of this, the integration of renewable energy such as solar thermal can cause difficulties in the convergence in the computational algorithm as energy consumers become producers reversing the flow through some parts of the network. Therefore, the challenge of this thesis is to consider the district heating network as a whole simulating every elements simultaneously: building energy consumption, solar thermal injection, seasonal storage and thermal losses in the network.

CitySim is already complete offering the possibility to study looped network with multiple heating stations considering solar thermal injections as well as seasonal storage. This thesis aims to further improve the previous work done on the development of CitySim and validate these impeovements applying the software on differenct case studies.

## 1.4 Thesis content

This thesis is composed of four distinct chapters.

Chapter 2 summarizes the original status of CitySim before starting this work. It introduces the different parts of the code in order to have a better idea of where the new implementations are inserted. The thermal model of the buildings of CitySim is discussed as well as the algorithm of convergence created by the former students Pierre Cognet. This will allow to establish the capacity of the computational framework already developed.

Chapter 3 gathers new implementations brought to CitySim in order to improve the simulations on high temperature district heating networks. It explains the implementation of the singular pressure losses and the functions implemented in order to simulate district heating networks with multiple heating stations.

Chapter 4 discusses the validity of the CitySim with two different case studies. The first validation is done on the branched network of Broc and the second one on the looped network of Verbier. For each of them, the hypothesis and benchmark are introduced in order to drive the validation. A discussion of these hypothesis on the basis of the comparison between the simulation and the measurement is carried out proposing new improvements of the computational framework in future works.

Chapter 5 presents the case study of the low temperature district heating network of Yverdon and the different extensions that are forecast in the coming years. The new implementations in order to be able to simulate these new district heating networks are firstly explained. Secondly, these new implementations are validated thanks to the scenario 2021. Thirdly, different scenarios have been considered in order to compare different connecting elements. The potential of the solar thermal has been investigated in the future extensions of the network. The optimization of the network using evolutionary algorithms could not be conducted as they were time consuming. Nevertheless, they will be presented in the oral that follows the delivery of the master thesis.

# CHAPTER 2

# ORIGINAL STATUS OF CITYSIM

CitySim is a widely used open-source physically-based simulation tool for the energy and comfort analysis at urban scale developed by the EPFL Home Solar Energy and Building Physics Laboratory LESO-PB. It aims to provide a decision support to urban energy planners and stakeholders in order to minimize the net use of non-renewable energy sources and thus the associated emissions of greenhouse gases. Based on a bottom-up approach, the software simulates dynamically on an hourly basis each element of an urban scene. These elements include buildings, solar panels, grounds, trees, and pedestrians. For this, the software needs among other things the 3D geometrical buildings, thermo-physical properties of the composites that make up these buildings, soil conductivity, tree species, climate file and so on. Results range from buildings' energy consumption, respecting the stochastic nature of occupants' presence and behaviour to surface temperatures estimating the urban heat island effect passing by the simulation of district heating network [17].

This section summarizes the original status of this tool before initiating to work on it.

## 2.1 District heating networks

District heating networks include three different components as shown in Fig.2.1: the heating station on the left hand side of the figure, the buildings on the right and the pipe network. The heating station is the producer that generates the heat. The buildings are the consumers that needs heat. The network connects the producer to the consumers bringing the hot fluid coming from the heating station to the different consumers satisfying their heat demand. The hot water is brought through the supply network (in red in the Fig.2.1). Once, its energy is depleted, the water goes back to the heating stations in order to be heated up again. In CitySim, the supply and return networks follow the same tracks but are simply shifted of a certain distance defined by the user. Thus, only one network is needed when building the input file for CitySim. The hot fluid transported by the pipes of the network do not supply directly the heat tanks of the consumer for private property reasons. Therefore, the network is split with a heat exchanger at the level of the consumer, as it is possible to observe it thanks to Fig.2.1. Usually, these networks are described by the terminology of primary. The primary network being the one going through the heating station and bring the fluid to the consumer and the second one being the network that only recovers the heat from the primary network and delivers the heat in the storage tank of the building. The heat is thus transferred through a heat exchanger named substation. Like this, the consumer keeps the possibility to be independent of the district heating network if he wanted to. A simplified schema of how it is represented in CitySim is given in the Fig.2.1.

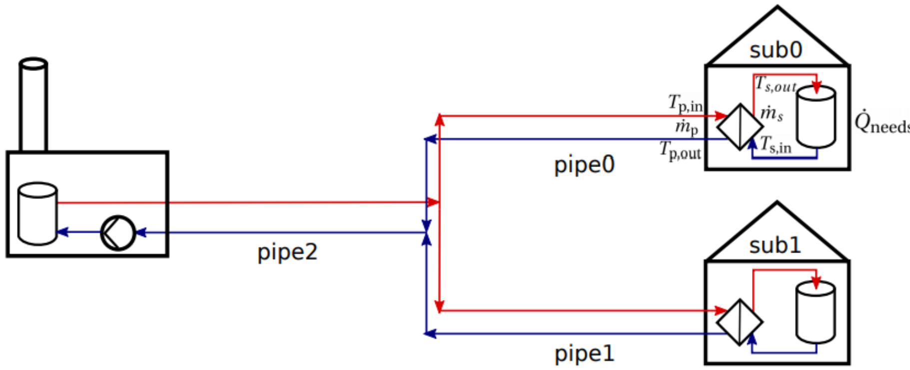


Figure 2.1: *Simplified schematics of a district heating network designed by Pierre Cognet.*

The part on the establishment of the energy demand of building as well as the solar thermal production was initially developed and validated by the Dr Jérôme Kämpf. The part about the network and the heating stations has been implemented and improved through the years by different students. The last one was Pierre Cognet and he has implemented the possibility to simulate complex networks as previously mentioned. Nevertheless, it was possible to simulate district heating networks with multiple heating stations only under very special conditions without any control on them.

## 2.2 Buildings

In CitySim, each building has its own thermal model. that asks to fulfill three different types of energetic demand: space heating (HS), space cooling (CS) and domestic hot water (DHW). HS and CS are adjused to maintain the temperature inside the building within a certain range. The demand of HS and CS is computed by considering various effects such as the irradiance of each facade, the thermo-physical properties of each walls (insulation, thickness, ratio of windows), the use of the blinds or the stochastic occupancy profiles. The DHW is estimated by defining a certain activity of DHW consumption. The occupancy profiles and activity types are given by the SIA standard according to the type of building simulated.

A water tank is associated with each of these energy demands. These tanks act as buffer in the simulations. It prevents heating or cooling systems to be turned on and off too frequently, which would reduce their efficiency. Each tank has a user-defined range of temperatures within which it aims to operate. The temperature of the tank decreases when it has to supply the building or increases when it has reached its lower bound and is supplied by the installed energy conversion systems.

In CitySim, the heat demand can be supplied using various energy conversion systems that have been already implemented as for example: the boiler, the CHP and the heat pump. For each of these technologies, the maximal power and efficiencies have to be set by the user. They are working in a pretty simple way. They supply the demand of the building until they reach their maximal power, and then they saturate. Solar thermal and PV panels can also be used as energy suppliers. They are allocated to the walls or roofs of the building. The operating mode of such devices is slightly more complicated, since the power they deliver depends on weather conditions. 2.3.

Evaluating the potential of solar thermal in district heating network, its operation is further explained. The solar thermal technology allows to retrieve the power coming from the sun thanks to what is called a solar collector. Many different types of solar collectors exist. They are split in two different families. There are either concentrating or non-concentrating panels. In both types, the principle is the same. There is a collecting area that is heated up by the sun. This part is then cooled down by using a working fluid, usually water. The water is then heated up and can be further injected in a building in order to deliver its heat. The non-concentrating panels are basically flat plates that are painted in dark and just collect the heat. The concentrating panels use mirrors in order to focus the rays from the sun in order to increase the power density. Thus, they can reach higher temperatures than their flat counterparts. They are consequently used more in the industry while the non-concentrating ones are used for residential heating. The implemented type of solar panel is thus belonging to the non-concentrating ones. The thermal power provided by each these devices is given by the equation (2.1),

$$\dot{Q} = \eta A G \tag{2.1}$$

where $\eta$ is the efficiency of the solar thermal panel [-], $A$ is the surface area of the collector [m$^2$] and $G$ is the solar irradiance on the panel [W/m$^2$]. The efficiency of the solar thermal panels is expressed by the formula (2.2),

$$\eta = \eta_0 - a_1 \frac{T_{fl.} - T_a}{G} - a_2 \frac{(T_{fl.} - T_a)^2}{G} \tag{2.2}$$

where $eta_0$ [-], $a_1$ [W/K/m$^2$] and $a_2$ [W/K/m$^2$] are parameters that are depending on each solar panels. These parameters are needed in the input file for the simulation and can be found usually with the manufacturer of the model that wants to be installed. $T_{fl.}$ and $T_a$ correspond respectively to the temperatures of the fluid and the air temperature, given in Kelvin. The temperature of the fluid $T_{fl.}$ is usually considered to be the arithmetic mean between the input and output temperatures of the fluid in the collector. The parameters $a_0$ and $a_1$ are strictly positive, meaning that the efficiency of a solar panel is decreasing with the temperature difference between the fluid and the air. It is easily understandable, since if the difference is big, more heat from the fluid will be dissipated to the environment. Consequently, according to the equation (2.2), it motivates even more the implementation of this device in low temperature district heating network. Indeed, for low district heating network, the temperature injected is at lower temperature which increases the efficiency of these solar panels. The formulas (2.1) and (2.2) are both implemented in CitySim and thus allow to compute the total energy given to the building by simply knowing which surfaces are covered of such technology. The water is then injected in the different water tanks introduced previously or directly to a district heating network thanks to the substation of type prosumer.

In the end, it is also possible to supply the heat demand thanks to a district heating network using the energy conversion system called substation. It is basically a counter current heat exchanger that allows to transfer the heat from the primary network to the secondary network as it is visible in the Fig.2.1. In order to perform some simulations with the substations, the following parameters are required.

- $linkedNodeId$ is the id of the node to which it is linked to in the network. It makes the link between the building and its location in the network.
- $P_{des.}$ is the design thermal power. It is the maximal power that can be delivered by the substation.
- $\Delta T_{des.}$ is the design temperature difference between the input and output on the primary side of the heat exchanger.

- $\epsilon_{des.}$ corresponds to the efficiency of the heat transfer in the heat exchanger at the design condition.

- *type* defines the type of substation and can either be "simple" or "prosumer" if the building is able to inject heat in the district heating network thanks to its own production or not.

Concerning the type "simple", the substation needs to satisfy the heat demand of the building, $\dot{Q}_{need}$. In a substation, it is assumed to always have the same temperature difference. Therefore, the primary side mass flow can easily be established according to the formula $\dot{m}_p = \dot{Q}_{need}/(c_p \Delta T_{des.})$. Regarding the type "prosumer", the establishment of its desired mass flow depends on whether it is a producer or a consumer. The operating mode of the prosumer, when it does not have enough solar thermal to supply its own heat demand, works as a "simple" substation. When the solar thermal panels are producing more heat than the one needed, the substation becomes a producer. Consequently, it starts to inject some hot water inside the network. It has been decided that the water was injected in the supply network at the global temperature setpoint of the network. The reason for this, is to prevent thermal rapid and frequent temperature variation that cause damages to the pipes and network components in the network. In addition, the other consumers do not need to be negatively impact by the injection of solar thermal. As an example, if the supply is colder from the rest of the network, the risk would be to lower the supply temperature for other consumers. The temperatures could go below the safe DHW temperature, which might cause health issues due to the proliferation of bacteria in the tank. The desired mass flow is hence established with the fraction of solar power that is left and the supply temperature. The return temperature is also a constraint, as it has no control on the upstream temperatures.

## 2.3 Network

In this section, the concepts of convergence in the network are introduced. In the C++ code, this corresponds to the functions $convergeHydraulic()$ and $convergenceThermal()$. These functions appear once the heat demand of each building has been established. Considering the case where there are no solar injection at first, the desired mass flow at each substation is known since the heat demand has been computed and as it is assumed to always have the same temperature difference $\Delta T_{des.}$. Therefore, the desired mass flow in order to satisfy the demand of each building is given by $\dot{m}_{des.} = \dot{Q}_{need}/(c_p \Delta T_{des.})$. These desired mass flows are the target at which the algorithm tries to converge to. Focusing on the convergence itself, two main steps can be distinguished. The algorithm successively performs the hydraulic convergence and the thermal convergence in order to find the physical solution that matches with the different desired mass flows.

### 2.3.1 Hydraulic convergence

Concerning the hydraulic convergence, the algorithm looks for the stationary solution. As seen previously, the changes in pressure or mass flows in the network travel at the speed of sound, which means that this hypothesis is thus quite robust since the algorithm finds a physical solution on an hourly basis. In order to perform this convergence, the network is decomposed in loops as shown in the Fig.2.2. The general idea of this decomposition is to simplify the problem. These loops are further called loopmassflows in order to distinguish them from the loops in looped networks. For each of the two loopmassflows in Fig.2.2, there is only one mass flow and the overall pressure difference has to be zero in order to find the stationary solution. Meaning that if they are pressure losses due to friction or valves, it has to be compensated by a gain in pressure difference with a pump. Hence, these pressure differences have to be of different signs. By convention, the pressure losses are positive, and the pressure gains are negative.

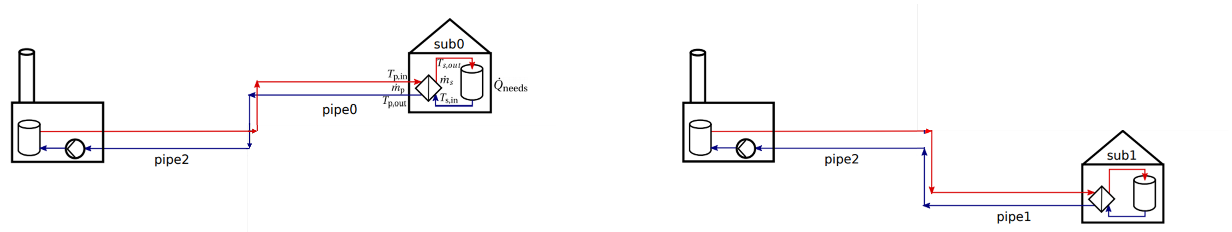


Figure 2.2: *Decomposition of the network in Fig.2.1 into several loops.*

Hence, the overall idea is that the heating station imposes a pressure difference thanks to a pump. The imposed pressure difference needs to be high enough in order to overcome all the pressure losses due to frictions between the flowing water and the pipes. Then, each substation can control the mass flow that they receive by choosing the opening of a valve to get the pressure drop corresponding to the desired mass flow. The valves and the pumps are hence control variables in the network that basically allow imposing mass flows or pressure differences at specific points of the network. For each hydraulic convergence, they have respectively a certain opening denoted by $K_v$ for the valves and a rotational speed $n$ for the pumps. With these, the pressure difference at each edges of the network can be computed knowing the mass flow of the pipe, $\Delta p_{edge}(\dot{m}_{edge})$. Therefore, the mass flow is adapted in the hydraulic convergence thanks to a slightly modified version of the NLEQ-RES Newton-Raphson method in order to have an overall pressure difference of zero for each loopmassflows. The system has considered to have reached convergence if in every loop, each residuals (i.e. the overall sum of the pressure difference inside a loopmassflow) is below 100 Pa. Of course, a maximal number of iteration, $n_{max} = 70$ has been set in order to avoid being stuck. As a comment, this hydraulic convergence could be further improved by using machine learning instead of the simple Newton-Raphson method. In fact, neuronal networks are well adapted in order to simulate district heating stations since the geometries of both are quite similar. An upcoming thesis by Roberto Boghetti will soon be carried out on this subject.

### 2.3.2 Thermal convergence

Once the hydraulic convergence is finished, the temperatures in the network are computed at each node (i.e. pipe connections, substations, or heating stations). The strategy in order to determine the different temperatures in the network is the following. First of all, it is supposed that the temperatures of the supply nodes are the same as those from the previous step. Then, starting from the substations, the temperature is propagated through the return network. This propagation of the temperature in the network is given by the pipe thermal model. This model allows to compute the temperature at the downstream end of the pipe, knowing the upstream temperature. This model considers three phenomena that can add or remove heat while the water is flowing though a pipe:

- Heat exchange with the exterior soil surface
- Heat exchange with the parallel twin pipe
- Heat exchange due to frictions between the water and the pipes

The computations of this downstream temperature are let to the reader since they have already been derived in [14]. The only change that has been done in this thesis according to the thermal losses is the use of the equation (2.3) in order to estimate the ground temperature given the buried depth of the pipes and the air temperature [15].

$$T(z,t) = T_m + A_s \exp -kzcos(\frac{2\pi(t-t_0)}{p} - kz) \tag{2.3}$$

where $z$ id the depth [m], $A_s$ is half of the amplitude of the hottest with the coldest one, $t-t_0$ is the time distance from the coldest day of the year $t_0$ [day], $p$ is the number of days in one year, $k$ is a factor considering the thermal diffusion coefficient. Having computed the downstream temperature, the thermal losses in each pipe is simply given by the expression $\dot{Q}_{loss} = \dot{m}c_p(T_{upstream} - T_{downstream})$.

Coming back to the propagation of the temperature, the temperature of the entire return network can be established using the following formula in order to compute the temperature at each node.

$$T_{noden} = \frac{\sum_{p \in \text{pipes with flow towards node } n} T_{downstream,p}\dot{m}_p}{\sum_{p \in \text{pipes with flow towards node } n} \dot{m}_p} \tag{2.4}$$

Once it is done, the same propagation is performed for the supply network starting from the heating station to the upstream temperature of the substation. This procedure is then repeated by computing the downstream temperature of the substation until the algorithm converges. The algorithm considers to have converged if all the upstream temperature of the substations of the step $n+1$ have a difference of 0.2°C with their counterparts at step $n$.

## 2.4 Heating stations

In CitySim, two different types of heating stations were already implemented. The first one called "simple" corresponds to the operation of a standard heating station. It is only composed of one pump that allows to create a target pressure gain. The control variable of this entity is thus a pump. The pressure gain due to the pump can be computed thanks to the following formula,

$$\Delta p_{gain} = a_0 \frac{n^2}{n_0^2} + a_1 \frac{n}{n_0}\dot{m} + a_2\dot{m}^2 \tag{2.5}$$

where the $a_i$ are characteristic parameters of the pump, $n$ the rotational speed, $n_0$ the nominal rotational speed and $\dot{m}$ the mass flow going through the pump.

Concerning the second type called "seasonalStorageHeating", the operating mode is slightly more complicated. As for the prosumer, the heating station with seasonal storage has two different operating modes. The first one is when the heating station delivers the heat to the network. The pump is used in order to supply the network from return to supply. In this case, the fluid is heated up by the energy conversion unit and the seasonal storage heating system. Nevertheless, when the prosumers in the network can supply themselves and the demand of the whole network, this heating station switched to the storage mode. Thus, the total mass flow is going from supply to return since the prosumers are injecting in the supply network. The mass flow coming in, is then injected in an isolated water tank and heats the stored water inside. The storage is used once the tank temperature is above the entering temperature. At this point, the water tank is used in order to preheat the fluid before going to the energy conversion unit of the heating station.

## 2.5 Overall control

In order to get a global picture of how the convergence is achieved in CitySim, the algorithm, 1 is displayed. The algorithm first looks if it has to update the desired mass flow or to update the operating mode of the seasonal storage heating stations, since the heating demand and desired mass flows have already been established. Knowing already the different desired mass flows, the valve openings, $K_v$, can be updated as well as the pump rotational speed, $n$. These updates are in the while loop of convergence, since the equations for updating $K_v$ and $n$ are both depending on the mass flow and pressure difference. The problem is that for the case of the valve, there is only a target for the mass flow and for the pump for the pressure difference. Therefore, they are computed using the ideal pressure difference and mass flow computed in the previous convergence step.

$$K_{v,ideal} = \dot{m}_{target}\sqrt{\frac{3600^2}{\rho_0 \rho}\frac{\Delta p_0}{\Delta p_{ideal}}} \tag{2.6}$$

$$n_{ideal} = n_0 \frac{a_1 \dot{m}_{ideal} - \sqrt{a_1^2 \dot{m}_{ideal}^2 - 4a_0(a_2 \dot{m}_{ideal}^2 - \Delta p_{target})}}{-2a_0} \tag{2.7}$$

The update of the desired mass flow of the prosumer substations and seasonal storage heating stations is also in the while loop, since the desired mass flow of the prosumer are depending on the return temperature. This return temperature evolves after each thermal convergence and thus change the desired mass flow of the prosumer. Consequently, the operation mode of the seasonal storage heating station could change if suddenly the total mass flow in the network is going in the reverse direction.

**Algorithm 1:** *Overall loop in order to converge to the stationary solution where all targets are satisfied.*

```
Function convergenceToEquilibrium(ρ, C_p, Climate, day, hour):
    k ← 0, notConverged ← true
    updateProsumerDesiredMassFlow()
    updateThermalStationOperationMode()
    while k < k_max and notConverged do
        // Update control variable positions
        valves.updateKv()
        pumps.updateN()
        // Make the system converged with the new control variables
        convergeHydraulic()
        convergeThermal()
        // Update the desired mass flows and operation modes
        updateProsumerDesiredMassFlow()
        updateThermalStationOperationMode()
        // Check for convergence
        e_rel ← computeRelativeError(substations, thermalPowerPlants)
        notConverged ← (max_i e_rel,i ≥ 0.02)
        k ← k + 1
    end
End Function
```

The system is in the end considered as converged if the mass flows for the substations and the pressure differences of the thermal stations are within a 2% of errors with their target value associated. For this thesis, the convergence criteria has been modified by introducing the absolute error. In fact, it has been noted that for cases where the desired mass flows were close to zero even the slight difference creates huge relative error. Therefore, an additional criteria has been implemented by looking at the absolute difference. In the end, with these two criteria, the cases with big or small desired mass flows are well treated. The threshold of the absolute error has been set at 0.002 kg/s. As a comparison, the measures on the mass flows given by Verbier have an uncertainty of the order of 0.025 kg/s.

## CHAPTER 3

## NEW IMPLEMENTATIONS IN CITYSIM

## 3.1 Implementation of singular pressure losses

The pressure losses in the network are a key element. They can be splitted in three different categories: the regular, singular and altitude pressure losses. It is important to take them into account especially for cases with multiple heating stations. Without them, the model could converge to non physical solutions which would be discussed in the section 3.2. The pressure losses are also essential for the establishment of thermal losses and electric consumption at the pumps.

The main contribution is coming from the regular pressure losses. This type of pressure losses is caused by the friction of the fluid with the pipe walls. It is happening since the fluid which has a finite viscosity encounters defects in the pipes. It creates a pressure drop that heats up the fluid because of the dissipation. Thanks to the work of Pierre Cognet, these regular pressure losses were already implemented. The pressure losses are approximated by the Weissbach equation.

$$\Delta P_{reg} = \frac{L f_D}{4\pi^2 \rho R^5} \dot{m}^2 \tag{3.1}$$

where $L$ corresponds to the length of the pipe [m], $R$ represents the radius of the pipe [m], $rho$ is the mass density [kg/m$^3$], $f_D$ the Darcy friction factor [-] and $\dot{m}$ the mass flow in the pipe. This equation considers the different regime of flow through the Darcy friction factor. The expression of this factor changes according to the reynold number which is given by the equation (3.2).

$$Re = \frac{2\dot{m}}{\pi R \mu} \tag{3.2}$$

where $\mu$ characterizes the viscosity of the fluid and is given by the semi-empirical Vogel-Fucher-Talmann relation.

The second type of pressure losses is the singular one. The regular pressure losses are for straight pipes but in reality there are curves, change of radius or T-junction in district heating networks. Singular pressure losses account for all these located changes. Despite all the different causes of singular pressure losses, the expression describing them is always of the same form.

$$\Delta P = K\rho \frac{v_i \cdot |v_i|}{2} = K \frac{\dot{m}_i |\dot{m}_i|}{\rho \pi R_i^2} \tag{3.3}$$

where $v_i$ is the speed of the fluid in the pipe $i$ which depends on the type of singular pressure losses, $K$ corresponds to a factor that varies according to the cause of singular pressure losses, $\dot{m}_i$ represents the mass flow in the pipe $i$ and $R_i$ is the radius of the pipe $i$ [18]. The absolute value has been used in order to keep the sign of the mass flow. This is the case because a pipe will always reduce the pressure, in the direction of the flow. Therefore, the pressure difference needs to be always of the same sign of the mass flow.

In this thesis, only two different types of singular pressure losses were implemented. The first one considered is the pressure losses caused by changes in radius pipes. The $K$ factor for the case of a shrinkage or an expansion are respectively given by the equation (3.4) [18].

$$K_{shrink} = 0.5(1 - (\frac{D_2}{D_1})^2) \qquad K_{exp} = (1 - (\frac{D_1}{D_2})^2)^2 \tag{3.4}$$

where $D_1$ is the internal diameter of the upstream pipe and $D_2$ is the internal diameter of the downstream pipe. Concerning the $v_i$, they are respectively the speed in the downstream pipe and upstream pipe for the shrinkage and expansion. These types of pressure losses are very small since the radius are decreasing gradually but they are very simple to implement as they did not require to modify the input file.In CitySim these pressure losses are computed together with the regular ones and are attributed to the pipes even though they occur at nodes. Attributing these pressure losses to the pipes instead of the nodes has the advantage of keeping the same size of the matrix that needs to be inverted. It spares then some time to not consider the nodes

The second type of singular pressure losses are the ones coming from T-junction appearing basically when three pipes meet. Two distinct cases have to be distinguished depending on the mass flows at the junction. There is first, the case where two mass flows join at the node and only is going out and the case where one mass flow is splitted in two. The expression of the $K$ factor are in both cases this time given in the table 3.1.

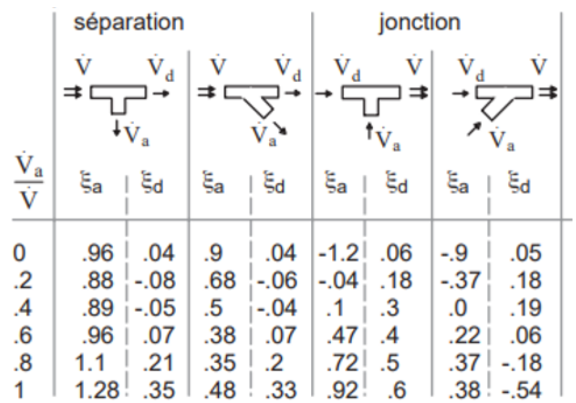

| $\dot{V}_a/\dot{V}$ | séparation $\xi_a$ | $\xi_d$ | $\xi_a$ | $\xi_d$ | jonction $\xi_a$ | $\xi_d$ | $\xi_a$ | $\xi_d$ |
|---|---|---|---|---|---|---|---|---|
| 0 | .96 | .04 | .9 | .04 | -1.2 | .06 | -.9 | .05 |
| .2 | .88 | -.08 | .68 | -.06 | -.04 | .18 | -.37 | .18 |
| .4 | .89 | -.05 | .5 | -.04 | .1 | .3 | .0 | .19 |
| .6 | .96 | .07 | .38 | .07 | .47 | .4 | .22 | .06 |
| .8 | 1.1 | .21 | .35 | .2 | .72 | .5 | .37 | -.18 |
| 1 | 1.28 | .35 | .48 | .33 | .92 | .6 | .38 | -.54 |

Figure 3.1: *Table displaying the K factor for different ratio of mass flows in the connected pipes having the same radius R. [18]*

where the $\xi$ in the table stands for the K factor in the equation (3.3). An interesting thing to note is that for some speed ratios the pressure loss are of the opposite sign of the mass flow. In specific cases, the split or the junction of mass flow are creating underpressurised pipes with respect to their neighbours which implies a suction of the fluid. These under pressurised local points are coming from turbulence and chaotic effects. In CitySim, an empirical function has been implemented in order to get the K factors by fitting the values in the table 3.1 with a quadratic function. The result of these fits are given by the following expressions.

$$K_a^{junc} = -1.6(\frac{\dot{m}_a}{\dot{m}})^2 + 3.6\frac{\dot{m}_a}{\dot{m}} - 1.1 \qquad K_d^{junc} = -0.14(\frac{\dot{m}_a}{\dot{m}})^2 + 0.7\frac{\dot{m}_a}{\dot{m}} + 0.039 \tag{3.5}$$

$$K_a^{split} = 0.74(\frac{\dot{m}_a}{\dot{m}})^2 - 0.42\frac{\dot{m}_a}{\dot{m}} + 0.94 \qquad K_d^{split} = 0.78(\frac{\dot{m}_a}{\dot{m}})^2 - 0.41\frac{\dot{m}_a}{\dot{m}} + 0.012 \tag{3.6}$$

In comparison to the previous singular pressure losses, they are a bit more complicated to implement. In fact, in the XML input file for the simulations, no information is given on the geometry of the pipes. Only the length and the id of which nodes the pipes are connected to, were provided. Finding the nodes where they are three connected pipes and it is a junction or a split are not a problem in the C++ code since the mass flows and the connected pipes are established before the computations of the pressure differences. The problem lies in distinguishing the pipe $a$ from the pipe $d$ of the Fig.3.1. The solution found in order to specify the pipe and attribute the correct pressure differences were to give two new attributes 'singular1' and 'singular2' for each 'Pipe' in the input XML file. They can be either 'straight' or 'T' depending if they are respectively the pipe $d$ or $a$ and the two attributes specifies on which nodes the T-junction is situated. Therefore, the code creating the input file for the simulation has been modified and a function computing the angles in between the different pipes on the basis of their geometry has been defined. In this work, the only singular pressure losses caused by T-junction considered are the one with a perpendicular connection of the 'T' pipe. In the future of course other types of singular pressure losses could be implemented but it makes no sense to go too much in details since the correction would be negligible in comparison to the error made from the uncertainty of insulation layers used in pipes, soil conductivity and other properties.

Concerning the last type of pressure losses due to altitude changes in the network, it has also been implemented by Pierre Cognet. These pressure differences, also known as static pressures differences, are not as important as the other two since they do not impact the convergence of the model. In fact, when the residuals i.e. the sum of the pressure losses and pressure gains through pumps, are computed the pressure changes due to the altitude change compensate with one another since the supply pipe and the return pipes have opposite difference of altitudes. Nevertheless, this type of pressure losses is interesting for certain district heating network as the one of Verbier. Indeed, the pipes and especially heat exchangers can not support too high static pressures. The operators of the DHN of Verbier speaks about a limit of 16 bars in their network. Consequently the extension of their dhn is limited to a certain range of altitude differences. The computations of this static pressure is very simple and given by the famous Bernoulli expression, $\Delta P_{alt} = \rho g \Delta z$ though it is very useful in order to prevent over pressurised heat exchangers or pipes which could cause dramatic damages in the network.

## 3.2 District heating networks with multiple heating stations

In district heating networks with multiple heating stations, some rules are needed in order to coordinate the different heating stations as the degree of freedom has increased. In fact, if no rule is implemented, the different heating might not work together but against each other unnecessarily increasing the usage of the pumps. Usually what is done in district heating network, they define a 'master' heating station that govern all the others that are commonly named 'slave'. This strategy of coordination of the different heating station is done through what is named a MCR which stands for "Measure Control Regulation". This summarizes the idea of controlling and regulating the different heating stations through measurements. This method reduces the degrees of freedom of the system and permit thus a better control of the different elements.

### 3.2.1 Measure Control Regulation

For this purpose, the class named MCR has been implemented in the C++ code. This class includes all the heating stations of the district energy center. They are sorted inside the vector in order to give the order of priority for them to changer their stage. The MCR is simply composed of one function called MasterControlSlave where the management of the heating stations is performed. In order to let the possibility to future developers of CitySim to implement other MCR, sub-classes have been created. The idea is to have one subclass for each MCR. The function MasterControlSlave would just have to be override in the subclass defining other strategies in order to manage the different heating stations.

In this thesis two MCR have been implemented. The first one represented by the subclass SingleMCR is the most basic strategy that exist where there is only one master heating station without slaves. The MasterControlSlave is in this case empty. The class only makes sure that the only heating station is not of the type slave. As a convention, it has been decided that a slave can not be ran without a master. The second MCR represented by the class SimpleMCR allows this time to control several heating stations together. In order to explain the rules that govern the different heating stations in a clearer way, the simple example where there are only two heating stations, one master and one slave, is taken. The instruction given to the slave is to simply start if the master is not able to supply the heat demand of the buildings anymore or in other words that it gets saturated. Then, the slave heating station starts and increase its power by steps in order to supply the missing heat demand. The master heating station then adapts its energy production in order to match the heating demand of the consumers. Considering discrete increase of the power in the case of the 'slave' allows to add some constraints reducing the degrees of freedom and thus have a simpler problem. Of course, this strategy can be generalised with multiple slaves. The slaves are then sorted defining an order of priority in order to update their stages. They are launched or stopped whether the previous heating stations have enough power to supply every consumers or not. It has been further decided to update only by one stage at each time step. As a matter of fact, the heating stations lose in efficiency if they are frequently changing of power. Reducing the variation of the slave ensures to run it at its optimal operation mode. This issue of optimal operation mode concerning the master is less important as it is supposed to be more powerful than its slave counterparts. Hence, the variations of its power in order to satisfy the heating demand are quite small compared to its nominal power. This problem of efficiency is even bigger when the heating station needs to start. In real cases, a heating station takes several hours in order to reach its optimal operating mode. Hence, it is not profitable to turn them on and off at each time step. For this purpose, a slave heating station has an internal time clock that prevents the slave to stop at a too close time step. This latency of the slave can be set by the user.

This rule is implemented following the algorithm 2 in CitySim.

**Algorithm 2:** *Establishment of the rules governing the heating station together.*

1 **Function** $AgentController(prevCurrentStages, \rho, C_p, day, hour)$**:**
2   **for** $i \leftarrow 1$ *to* $nThermalstations$ **do**
3     // Establish the total power available with the previous heating station
4     $P^{max}_{avail.} \leftarrow thermalstations.getThermalPowerMax(i)$
5     // Establish the total power needed
6     $P^{Needed}_{tot.} \leftarrow thermalstations.getThermalPowerNeeded()$
7     // Update the stage of the slave
8     $thermalstations[i].updateStage(P^{max}_{avail.}, P^{Needed}_{tot.}, prevCurrentStages[i],$
9         $\rho, C_p, day, hour)$
10   **end**
11 **End Function**

In the algorithm 2, every slave heating stations have their stage that is updated thanks to the function *updateStage*() on line 10. Consequently, the **for** loop starts at one since the first element of the vector is by convention the master. The variables $P_{avail.}^{max}$ and $P_{tot.}^{Needed}$ are needed in a further establishment of the desiredStage at which the slave wants to be. The same would have been possible with the thermal provided of the previous heating stations by calling the function $getThermalProvided()$. Nevertheless, $P_{avail.}^{max}$ is preferred as it is fixed during the convergence. It allows to have more robust convergence. Regarding the boolean $prevSlaveShutDown$, it ensures that the $ith$ slave heating station does not power up if the previous heating station get shutdown. These cases are possible since the slave heating station might not be shut down even if it should with respect to $P_{avail.}^{max}$ and $P_{tot.}^{Needed}$ due to the latency imposed. The $prevCurrentStages$ are the stage of the heating stations at the previous time step. This variable is useful since it has been decided to constraint the slave heating stations to jump only one stage per time step.

Looking now at the implementation of the heating stations in CitySim, new types have to be incorporated in the C++ code. In the case of the master heating station, its operation is very similar to the operation of the heating station of type 'simple' explained in the section 2.2. Therefore, no additional entity has to be created. However for the slave heating station, the implemented heating stations do not apply since the power of the slave has to be controlled. The Fig. 3.2 represents the schematics of this slave heating station.

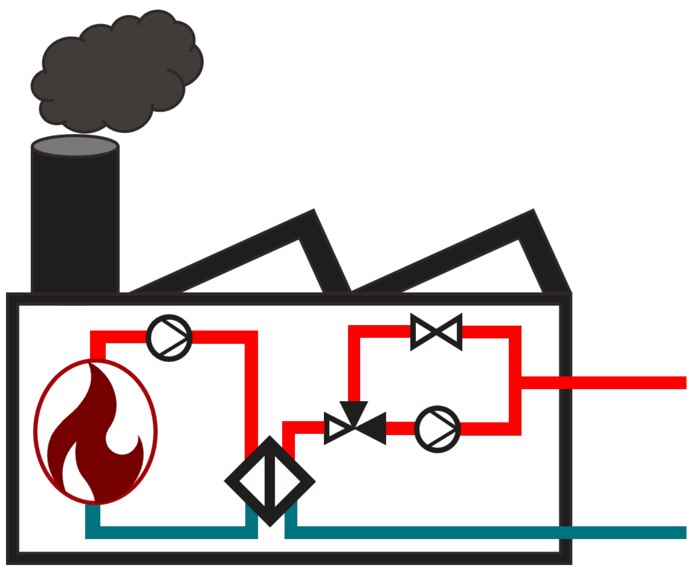

Figure 3.2: *Schematics of the hydraulic model of the slave heating station. When the thermal station supply the network, the three-way valves connect the heat exchanger to the pump, leaving the valve unused. In that case, the flow goes from return to supply and the three-way valves help the pump to control the mass flow. When the thermal station is shut down, the three-way valves connect the heat exchanger to the valve that prevent the flow to go from supply to return.*

### 3.2.2 Slave heating stations

In CitySim, the slave heating station appears in a new class called ThermalStationSlave which is a subclass of ThermalStation. The novelty in this heating station lies in the fact that the power delivered is controlled and evolves in time by step. This heating station has as well a target temperature at which the fluid exits the heating station. In order to not impact negatively the other consumers when the slave heating station gets started, the flow exiting the slave has to be at the same temperature as the one from the master. In fact, problems could arise if the slave injects the fluid at colder temperatures as it could lower the overall supply temperature. This could be harmful for certain consumers as bacterias can proliferate in DHW tanks if the temperature is below the threshold of 60°C. In this problem, the return temperature is also a constraint as it can not control the upstream temperature of the fluid arriving from the rest of the network. In the end, with these three constraints, the power can be controlled through its mass flow. The equation (3.7) gives the relation between those two variables.

$$\dot{M}_{des.} = \frac{desiredStage \cdot \dot{Q}_{max}}{c_p(T^{target}_{supply} - T_{return}) - \frac{\Delta P_{pump}(1-\epsilon_{pump})}{\rho \epsilon_{pump}} - \frac{\Delta P_{valve}}{\rho c_p}} \tag{3.7}$$

This equation is simply derived from the famous expression $\dot{Q} = \dot{m} c_p \Delta T$ taking into account the heat supplied by the pump and the valve due to frictions with the flow. One can note that the desired mass flow depends on the return temperature and on the pressure differences of each control elements. These variables are all depending on the mass flow which means that the desired mass flow has to be updated after each thermal equilibrium cf. algorithm 1. The update desired mass flow does not require to be damped with the Robbins-Monroe annealing solution since the control variables $K_v$ and $n$ are already using it avoiding to be stuck in cycles during the convergence.

This desired mass flow is therefore set in the function *updateStage*() of the ThermalStationSlave.

**Algorithm 3:** *Establishment of the stage for the further step.*

**Function** *updateStage*($P^{max}_{avail.}, P^{Needed}_{tot.}, prevCurrentStage, \rho, C_p, day, hour$)**:**
  $nextStage \leftarrow currentStage$
  // Establishment of the desired stage
  $desiredStage \leftarrow \frac{P^{Needed}_{tot.} - P^{max}_{avail.}}{getThermalPowerMax()}$
  // Upgrade of the current stage
  **if** $desiredStage > currentStage$ **then**
    $nextStage \leftarrow upgrade(prevCurrentStage)$
  **end**
  // Downgrade of the current stage
  $underStage \leftarrow downgrade(prevCurrentStage)$
  **if** $underStage < currentStage$ **then**
    $nextStage \leftarrow underStage$
  **end**
  // Do not shut down the slave
  **if** $nextStage == 0$ *and* $timeClock > 0$ **then**
    $nextStage \leftarrow rampingStages[1]$
  **end**
  $currentStage \leftarrow nextStage$ $setDesiredMassFlow(\rho, C_p, day, hour)$
**End Function**

In the algorithm 3, the first two conditions set the stage for the next steps. As discussed previously, these changes are limited to only one stage per time step. Concerning the last condition, it simply prevents the slave heating station to be switched too rapidly after being switch on. Setting the desiredMassFlow, it is now possible to update the control variables in order to make the code converged to this target.

The update of the control variables is slightly more complex since a ThermalStationSlave when switched on is composed of two different control elements, a pump and a valve. Even though, it seems that the two control variables go together since one is used in order to reduce the pressure and the other one in order to increase the pressure. However, even for real cases, the valve helps the pump to control the mass flow going through it. The slave heating station has still a target pressure difference in order to compensate the pressure losses in the network and therefore it has to be splitted through the different control elements. There are then two different target pressure differences for the valve and for the pump that summed up have to be equal to the total target pressure difference, $\Delta P_{target} = \Delta P^{valve}_{target} + \Delta P^{pump}_{target}$. The update of the $K_v$ and the $n$ are then computed by accounting for the pressure difference of the other control variable as it is shown in the algorithm 4.

**Algorithm 4:** *Establishment of the update of the control variable for the slave heating station.*

**Function** $updateControlVariable(\Delta P_{target}, \rho, T_{in}, learningRate)$:
- **if** $\dot{M}_{des.} > 0$ **then**
  - // The heating station needs to be on.
  - // Set the Rpm of the pump and the $K_v$ of the valve in order to have $\Delta P_{target}$ around the substation.
  - $\Delta P^{pump} \leftarrow pump.computePressureDiff(\dot{M}_{des.})$
  - $\Delta P^{valve}_{target} \leftarrow -\Delta P_{target} + \Delta P^{pump}$ Opposite signs due to conventions
  - $valve.updateKv(\rho, learningRate, \dot{M}_{des}, \Delta P^{valve}_{target})$
  - $\Delta P^{valve} \leftarrow valve.computePressureDiff(\dot{M}_{des.}, \rho)$
  - $\Delta P^{pump}_{target} \leftarrow \Delta P_{target} - \Delta P^{valve}$
  - $pump.updateRpms(learningRate, \dot{M}_{des.}, \Delta P^{pump}_{target})$
- **else**
  - // The heating station needs to be off. Shutdown the valve.
  - $\dot{M}_{des.} \leftarrow 0$
  - $valve.updateKv(\rho, learningRate, \dot{M}_{des}, abs(\Delta P_{target}))$
- **end**

**End Function**

When the heating station needs to be turned off, a valve is still needed in order to make sure that the flow does not go on the opposite direction. It has been decided to not implement this valve in order to avoid this reverse mass flow for the master heating station since it is not supposed to be shut down. Nevertheless, the user has to be careful when setting the different heating stations. In fact, it has to make sure that the pressure difference at the master heating station can not be overcame by the slaves. This situation is not supposed to happen in real cases since the master is the strongest heating station.

### 3.2.3 Overall control

A new version of the algorithm 1 is required as shown in algorithm 5. As previously mentioned, the slave heating stations must adapt the desired mass flow depending on the temperatures at its return node. Thus, this update needs to be done at each step in a similar way as the prosumers.

However, the redistribution of the work between the heating stations through the function $MasterControlSlave()$ is called only after the first iteration as it needs to evaluate the thermal power asked to the heating stations.Therefore, the desired mass flow of the slave heating stations is set after the first iteration meaning that the learning rate will be below one which will damp the changes of rotational speed of the pump from the slave heating stations.

**Algorithm 5:** *Overall loop in order to converge to the stationary solution where all targets are satisfied. Similar to algorithm 1 but adapted for the MCR.*

**Function** $convergenceToEquilibrium(mcr, \rho, C_p, Climate, day, hour)$**:**

  $k \leftarrow 0$, $notConverged \leftarrow true$

  $updateProsumerDesiredMassFlow()$

  $updateThermalStationOperationMode()$

  **while** $k < k_{max}$ *and* $notConverged$ **do**

    // Update control variable positions

    $valves.updateKv()$

    $pumps.updateN()$

    // Make the system converged with the new control variables

    $convergeHydraulic()$

    $convergeThermal()$

    // Update the desired mass flows and operation modes

    $mcr.MasterControlSlave()$

    $updateProsumerDesiredMassFlow()$

    $updateThermalStationOperationMode()$

    // Check for convergence

    $\vec{e}_{rel} \leftarrow computeRelativeError(substations, thermalPowerPlants)$

    $\vec{e}_{abs} \leftarrow computeAbsoluteError(substations, thermalPowerPlants)$

    $notConverged \leftarrow ((max_i e_{rel,i} \geq 0.02)$ or $(max_i e_{abs,i} \geq 0.002))$

    $k \leftarrow k + 1$

  **end**

**End Function**

# CHAPTER 4

# VALIDATION OF THE CITYSIM TOOL

This chapter aims to validate the previous and new implementations done in the computational framework using case studies. It exists several methods to validate a software like CitySim depending on the data available and the complexity of the model studied. The validation tools that are available are the following.

- Plausibility check on toy networks
- Validation on measured data on real case studies
- Comparison with other software

Concerning the plausibility check, the major advantage of it is that it is always available. This validation can be carried out with existing network as well as fictive networks. Hence, it is very useful in testing new implementations. Most of the time, new implementations are not even doing what they were supposed to do. Therefore, inventing simple toy networks allow verifying what is really happening directly in the code. This method has always been used in order to validate the new implementations, even though they are not figuring in this work. The drawback of this validation tool is that it provides approximate results. Only the general idea is given. In addition, the plausibility check is highly dependent on the toy network chosen by the developer. Sometimes, the network could even be non-realistic. As an example, it has been tested a network with two heating stations that are close one to another with only one consumer. In this case, the algorithm was having troubles in order to converge since the two heating stations were competing with each another. In real cases, multiple heating stations are usually implemented in looped networks.

Regarding the validation with measured data on real case studies, it allows a precise validation of the model. This method is usually used in a second time after the plausibility check. This kind of validation is essential in order to prove the efficiency of the computational framework to the scientific community [19]. Nevertheless, this type of validation has many drawbacks. The first of them is that a case study is needed with robust data, which is pretty rare. Usually, the operators have no use to take frequent measurements of data. In addition, if data were measured, they are usually not stored for a very long time. The other challenge that represents the simulation of a case study is the gathering of all the necessary information such as the layout of the network, the nominal diameter of the pipes, the characteristics of the pump among other things. The bigger the network, the more difficult it is to get correct data. Sometimes, the operator themselves do not know where to look to get the information. Another problem that might occur while studying real cases is the appearance of non-predicted events such as the maintenance of certain parts of the network or the manual activation of heating stations overcoming the rules. Thus, the contact between the operators and the developers of simulation tools is crucial in order to explain the differences between the simulation results and the data measured.

The last validation tool can also be very helpful for the validation of a computational framework. In fact, many software programs are also simulating networks, such as pandapipes or ESP-r. However, it is not always straightforward to compare one network with two different models, as the inputs of each model are different. In addition, one of the two software has to be previously validated using case studies. This type of validation has not been carried out in this work, but would be useful in a future work.

## 4.1 Results of CitySim simulation on case studies

In this part, CitySim is validated thanks to two case studies. The first one is a simple-branched district heating network with a single heating station. This case study has already been studied by Pierre Cognet which validated his implementations on it. The second case study is more complex and allows to test the algorithm on loop networks with multiple heating stations. The benchmark used in order to evaluate the performance of the simulation in each case studies depends on the data available. For both case studies, the energy consumption of each substation was known. This energy demand from the building was imposed at the substation in order to remove the errors due to the building simulation. It allows to evaluate the performance of CitySim to simulate the district heating network only.

### 4.1.1 Broc: Branched network with a single heating station

The first case study discussed the district heating network of Broc. It is a rather simple branched network. The topology of the ground is flat for most of the part of the network. There is only one heating station in the network supplying 43 buildings. This network shown in Fig.4.1 had already been investigated by Pierre Cognet in order to validate the implementations done for his thesis. Consequently, the same input XML files for the simulation have been taken, checking the validity of the new implementations and minor corrections done in the C++ code.

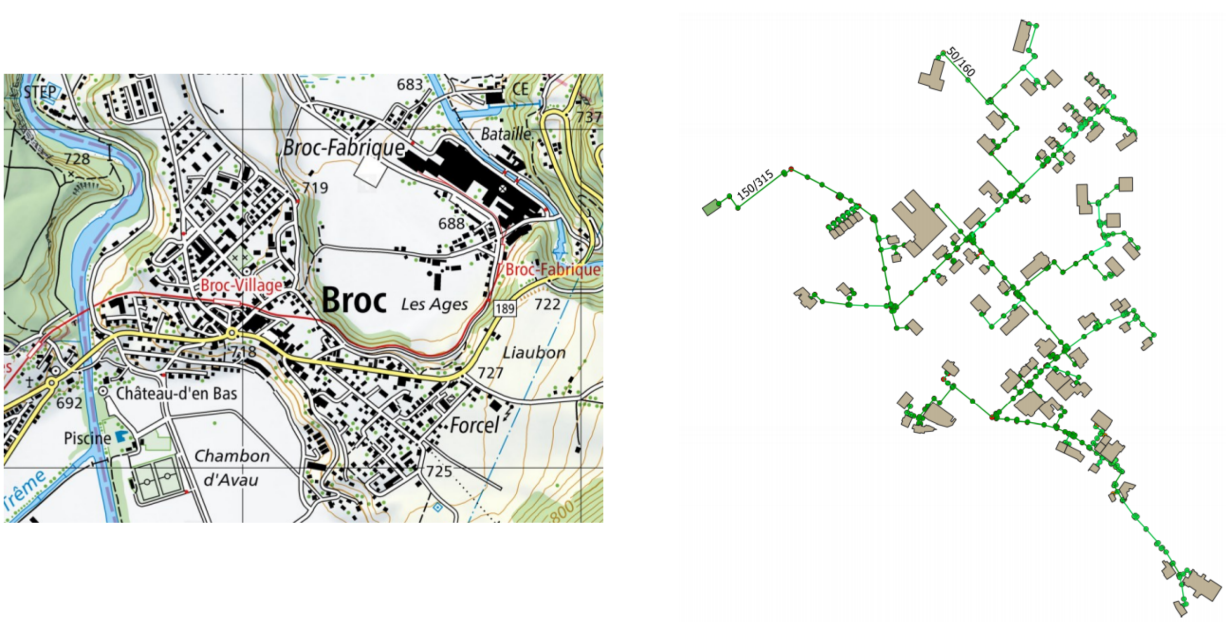


Figure 4.1: *Topographic map of Broc (left) and the QGIS visualisation of the district heating network with consumers in grey and the heating station in green in 2019 (right) [14].*

### Hypothesis and benchmark

For this validation, some hypotheses have been chosen in order to constrain the problem and some measured data provided by the operators of the network have been used as benchmark for the evaluation of the simulation performance. The same hypotheses and benchmark as the ones from Pierre were expressed.

Regarding the hypotheses made on the network, the first one concerns the exiting temperature of the network. A target temperature is set following the external temperature. The idea is to be hotter in winter than in summer, since it has usually more thermal losses, giving the lower ground temperatures. Therefore, the heating station ensures that the most disadvantaged building in the network has still water above 60°C avoiding the legionella proliferation. Following the same concept, the pressure setpoint around the pump at the heating station are linear by parts. The pressure difference around the pump increases according to the mass flow going through. This is done in order to compensate the higher pressure losses in the network due to frictions with the internal walls of each pipe. In the end, the difference of temperature between the incoming and exiting flows, $\Delta T_{des.}$, is supposed to be constant throughout the simulation. This value is imposed in order to reduce the degree of liberty of the equation (4.1).

$$\dot{Q} = \dot{m} c_p \Delta T \tag{4.1}$$

In the expression (4.1), the $\dot{Q}$ is known as it is given either by the software that computes the energy demand of the building or by imposing the heat demand measured. Talking about the power consumption, the data provided by the operators were updated every 100 kWh recording. The time was recorded after each up. This approximation deteriorates the data, as the consumption is not linear during the day. Thus, the power was smoothed on the daily average. The heat capacity $c_p$ is also known as water is flowing in the pipes. It remains thus one degree of liberty. As discussed in the section 2.2, the substation control the mass flow using a valve. It is then convenient to compute a desired mass flow on the basis of this constant $\Delta T_{des.}$, even though it is in reality non-constant. Since no data were provided regarding the temperatures at the substations, the same $\Delta T_{des.}$ is applied for every substation. It is computed by looking at the mean difference temperature at the heating station. The corresponding difference temperature is $\Delta T_{des.} = 22$°C. [14]

Moving now to the benchmark used for the validations, they are given by the following list.

- Entering and exiting temperatures at the heating station
- Mass flow going through the heating station

These data were provided in the period going from the 2nd of October 2018 to the 23rd of January 2019. These measurements together with the energy consumption of every building allow to compare the thermal losses, which becomes a fourth benchmark for the evaluation of the performance of the simulation. Despite the low number of benchmarks, they are at least at the heating station, which allows to have a global picture of the performances of CitySim. The main criteria for the validation of this case study is the entering temperature at the heating station. This variable is the one that is the furthest from the initial point. In fact, the flow had to go in the entire network before to come back.

### Results

Compared to the thesis of Pierre Cognet, the results are different due to the method of computations of the desired mass flow. In the previous work, the method going by step was used. This method allows to have faster convergences, but it gives results that are less precise with respect to the target that was fixed. Indeed, the computed desired mass flow overestimates the one actually required with the design temperature difference. In the work of Pierre Cognet, a $\Delta T_{des.}$ has been set at 30°C which is as expected too high according to the measurements of the temperature difference at the heating station. But then it will anyway set a higher desired mass flow because of the steps and will thus decrease the temperature difference. In the end, the choice needs to be carefully done depending on each case. In the case of Broc, it can be noted from the Fig. 4.2 that the temperature difference at the heating stations is not constant. Therefore, the method with steps has been preferred, but it is not always the case. As it will be seen with the case study of Verbier, the other methods have been taken.

The results given by the simulation are shown in the Fig.4.2 and Fig.4.3.

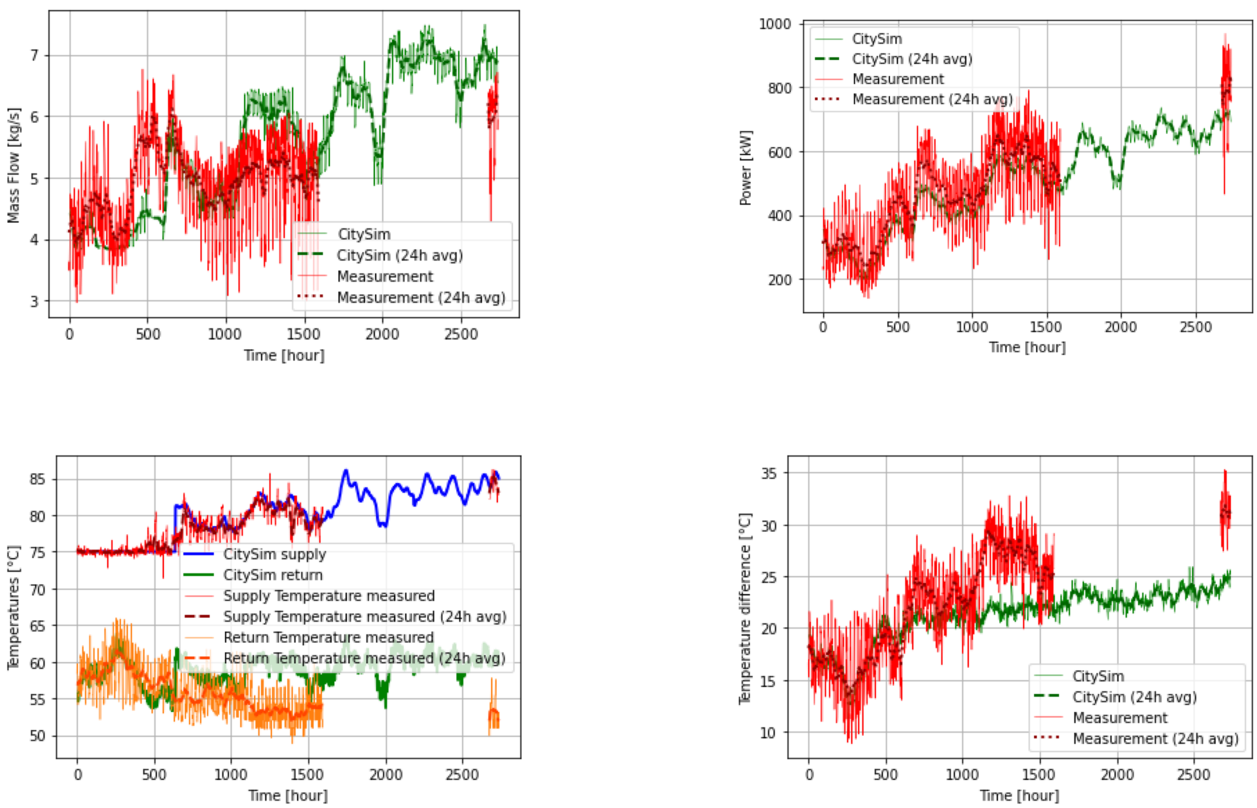


Figure 4.2: *The comparison between the CitySim simulation and the measurement at the heating station for the mass flow, the power delivered, the entering and exiting temperatures (middle), and the temperature difference starting on the 1st of October 2018 at midnight.*

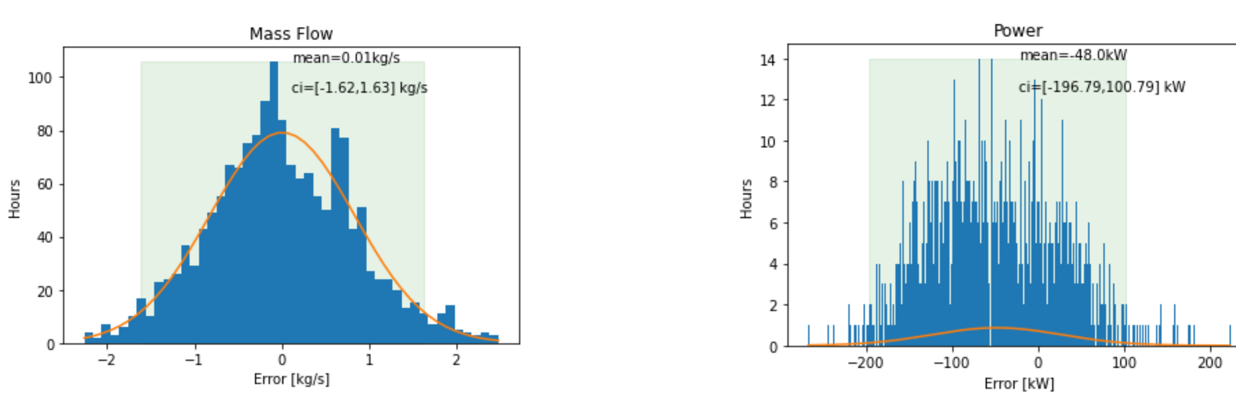

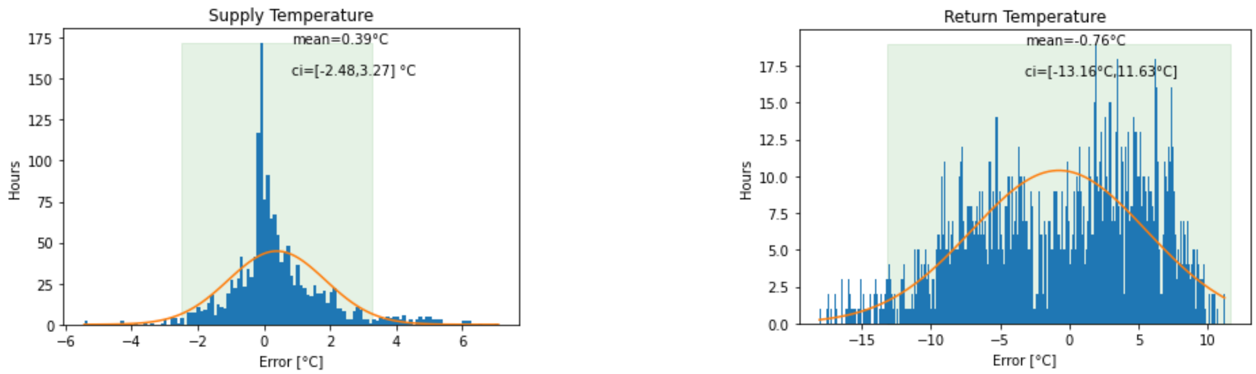


Figure 4.3: *Distribution of the absolute error between the CitySim simulation and the measurement on the mass flow, the power delivered and the exiting and entering temperatures at the heating station starting on the 1st of October 2018 at midnight.*

From both figures, it is possible to observe the quality of the simulation results on the different benchmarks. Considering the mass flow, the mass flow is correctly estimated at the beginning, but differences occur afterward. The first big difference appears when the heating station switches from summer to winter mode. This error comes from the fact that the target supply temperature is directly reached with the simulation, as no inertia of any kind is considered. As the simulation has as the objective to fulfill the imposed heat demand, the mass flow decreases as the $\Delta T$ is bigger. Then, new differences occur afterwards as the temperature difference is increasing reaching the implemented 30°C. Therefore as explained previously, the mass flow is always overestimated accordingly to the design temperature difference due to the step function. Therefore, when the measured temperature difference reaches 30°C, the mass flow is higher as it is visible in the Fig.4.2. In the end, the mass flow has a 95% confidence interval of [-1.62,1.63]kg/s. Concerning the power, it is quite well estimated. Looking, in the thesis of Pierre, one can notice that the imposed heat demand at the different building was well satisfied. Consequently, it is not surprising to have correct overall power consumption since the difference are only coming from the estimation of the thermal losses. The confidence interval is nevertheless going from -197 kW to 100.8 kW because of the oscillations caused by the inertia of the energy conversion system that is always adapting its power in order to satisfy the demand. Regarding the supply temperature, the confidence interval is only of a few degrees. The only differences are caused by the fact that the energy conversion system of the heating station, as it takes some time to get the next target temperature. Finally, the return temperature is where the difference is the highest, which is normal as it is computed by using the supply temperature and the mass flow in the end. The difference is big, as the formula that drives the heat exchanger is not known and is approximated. The analysis of these benchmarks will not be treated in further details, since the implementation of the singular pressure losses did not have changed the results with respect to the thesis of Pierre Cognet.

### Conclusion

As a conclusion, the results given by CitySim for the case study of Broc are acceptable according to the hypotheses made on the temperature difference at each substation. The return temperature is particularly impacted by this. Therefore, it has been identified the need of finding a new rule for the heat exchanger. In the other case study, the other method will be tested, but it is still quite simple according to what is really happening in the substation. In order to simulate this entity in a more precise way, the secondary network has to be simulated too and the rules that are governing the opening of the valves have to be established.

### 4.1.2 Verbier: Looped network with multiple heating stations

Since the case study of Broc has poor data precision and is a rather simple network, the need of finding a more complex network is essential in order to validate CitySim. In this context, the case study of Verbier allows to have a rather complete database, and the opportunity to test the tool on looped networks with several heating stations. This network visible in Fig.4.4 is situated in the Swiss alps in the famous ski resort of Verbier. This network is lying on the slope of the mountain. This is not supposed to change fundamentally the hydraulic convergence as previously mentioned in the section 3.1, but it allows testing in the meantime networks that are not flat. This network is composed of one loop and had, in the period considered for the study, two heating stations. The main one named the Trois Rocs and the smaller one called Mondzeu.

The district heating network of Verbier is expanding rapidly, and many extensions are forecast, as well as implementation of new heating stations. Hence, the operators are interested in knowing how to handle the different heating stations in their network. For this study, it has been chosen to consider the network in the first month of 2019 since the data provided by Altis, the private company monitoring the district heating network, were for this period.

#### Geographical data

At the beginning of this work, the data available on the PostgreSQL were incomplete and inconsistent with data coming from the CREM. Therefore, the network has been designed from scratch with the help of Altis and the CREM. Since the topology of the network is pretty complex, python files have been created in order to look for inconsistencies in the data provided by the different source of information. An example of one of the solution found is displayed in Fig.4.15. In addition, as the nomenclature of building id was proper to Altis, it has been necessary to exchange with them in order to get the correct id. This results in the following layout of the network, but given the difficulty of obtaining these different data, and the lack of consistency in those that were provided along my internship, the model could still have some errors.

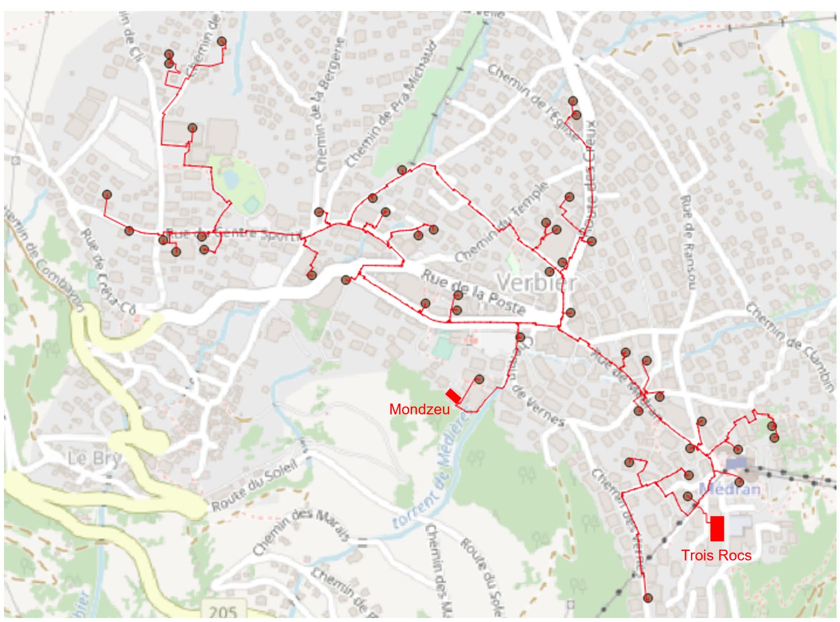


Figure 4.4: *Map of the district heating network of Verbier in 2019.*

On the Fig.4.4, the district heating of Verbier in 2019 is represented with the two heating stations in red. One can notice that on the Fig.4.4, there is only one network drawn. This is simply due to the fact that in CitySim, the supply and return networks are considered as identical but shifted of a certain distance defined by the user.

The data used for this study were pushed to a new PostgreSQL database in order for users of the CitySim tool or other equivalent software to be able to retrieve or compare the results obtained. The data allowing to build the network are classified in three distinct tables.

The first one gathers all the data related to the pipes.

| | altitude character varying | id bigint | dn bigint | length double precision | geometry geometry | start_point_id integer | end_point_id integer |
|---|---|---|---|---|---|---|---|
| 1 | [1470.248565522721, ... | 0 | 200 | 12.0312143101919 | 010500008001000... | 0 | 1 |
| 2 | [1470.248565522721, ... | 1 | 200 | 12.0065061140442 | 010500008001000... | 1 | 2 |
| 3 | [1470.248565522721, ... | 2 | 200 | 11.9605864293277 | 010500008001000... | 2 | 3 |

Figure 4.5: *Table containing information related to the pipes in the PostgreSQL database on the network of Verbier in 2019.*

In the table 4.5, the first column *altitude* represents for each pipe the altitude at each change of direction of the network. This data is unfortunately not really reliable since the data were not already available from Altis. It would have been necessary to use the database of SwissAlti3D in order to get the topology of the ground and to further estimate the altitude of the different pipes. As this procedure is quite time demanding, it has not been performed in this work. The following four columns correspond respectively to the id, the nominal diameter, the length, and the geometry of each pipe. The geometry of the pipes are stored in their hexadecimal form.

The second table been pushed to the PostgreSQL database, provides information about the location of the different nodes in the network. It mainly allows to link the network with the different buildings. This table is displayed in Fig.4.6.

| | point character varying | altitude double precision | idpoint integer | home_id double precision |
|---|---|---|---|---|
| 1 | 010100008050022A23... | 1470.24856552272 | 0 | NaN |
| 2 | 0101000080806 8FC3E... | 1470.24856552272 | 1 | NaN |
| 3 | 010100008060636C5A... | 1470.24856552272 | 2 | NaN |

Figure 4.6: *Table containing information related to the nodes in the PostgreSQL database for the network of Verbier in 2019.*

The first column corresponds to the geographic location of the node. It is then possible to create QGIS visualisation of the network. The altitude of each point appears in the second column. The third column designates the id of the point and corresponds to the ids displayed in the last two columns of the Fig.4.5. Finally, the *home_id* indicates if the node is connected to a building or not.

The last database provides the information regarding the two heating stations of the network. The first column gives the names of the heating stations. In this case, the names are Trois Rocs and Mondzeu. Then, the node id at which the heating station is connected appears. The last column gives an indication on the altitude of the two heating stations. The structure of the table is very similar to the previous ones, and hence it is not given.

### Hypothesis and Benchmark

In the same idea as for the case study of Broc, some hypotheses have been made for the simulation to run, and the measured data provided by Altis were used as benchmark.

In comparison to the case study of Broc, the data of Verbier were much more accurate than the one provided by the operators of Broc. The measurements recorded were also more diversified in the network allowing a robust validation of the computational framework developed. Thus, the benchmark used for the validation are the following.

- Entering and exiting temperatures as well as the mass flow at each substation
- Entering and exiting temperatures as well as the mass flow at the heating station of the Trois Rocs

These data were provided for the whole year of 2019 concerning the substations and only from the 1st of January to the 28th of May 2019 for the heating station of the Trois Rocs.

Concerning the hypotheses, the first one concerns the temperature difference at the substation. Once again, it is considered constant. The establishment of the temperature difference is computed in the same way as before by looking at the temperature difference between the entering and exiting temperatures at the main heating station of the Trois Rocs. Consequently, the value of 30°C is considered for every substation in the network. Regarding the heating stations, only few data were given on the second heating station of Mondzeu. The only indication was its nominal power. Furthermore, the operation of Mondzeu at the time was updated manually without looking for a specific rule governing the division of the workload. Hence, the use of the MCR implemented in CitySim will be applied. This allows in the meantime to perform a further validation. According to the indication of Altis, the heating station of Mondzeu is operated less than 1000 hours per year. Hence, the Trois Rocs is defined as the master heating station and Mondzeu is the slave. The thermal power of both heating stations are set to 2 MW. For simplicity, the pressure difference around the pump of the heating stations are kept constant. Therefore, they have been defined at their maximal pressure difference, which are 2.4 bars for the Trois Rocs and 3.0 bars for Mondzeu. Moving to the properties of the pump, only the characteristic curve of the pump of Mondzeu was available. Concerning the pump of the Trois Rocs, the same characteristic as the one from Broc has been used for the simulation. Finally, for the exiting temperatures, no rules were identified for both heating stations. Consequently, they have been imposed for the master in the same way as the heat demand is imposed for the substations and for the slave a constant temperature of 82°C has been set. The choice of 82°C is given by the range of temperatures at which the Trois Rocs supplies the network. In fact, it is preferable to have similar exiting temperatures, as it prevents the proliferation of the legionella. Moreover, being at similar temperatures reduces thermal shocks in the pipes.

In parallel to this thesis, a MQTT connection between the database of the operators of the district heating network of Verbier and the database of kaemco has been done. Thanks to this connection, in the future, the data will be transmitted on a continuous basis, preventing data losses between the partners.

**Results**

In this paragraph, the different comparison between the measurements and the simulations are displayed. In the different time evolution, the daily average is always also computed, since the simulations do not have inertia. They look for a stationary solution as explained in section 2.3.1 while in real life, the heating unit is always adapting itself to new energy demand. Hence, it is constantly moved from a stationary state. Nevertheless, the daily average smooths these oscillations, allowing to study the differences. As a difference from the previous case study, it has been decided to use the full proportionality in order to get the desired mass flow at the substation since the temperature difference at the heating station is rather constant through the period of the study, as it is possible to see from the Fig.4.7.

Starting with the heating stations, the first thing to notice is that the Mondzeu heating station is never started. Unfortunately, the heating station of the Trois Rocs is always powerful enough in order to fulfill the energy demand of all consumers. The network is then only testing a loop topology with one heating station. However, a variant of the network of Verbier will be studied later on in order to validate the MCR implemented. The comparison of the supply temperature is also not displayed, since it is used as an input by the program. Thus, only the mass flow and the return temperature are compared with the measurements together with the power delivered by the heating station. The Fig.4.7 and 4.8 show this comparison of the evolution of those two variables and the error between them.

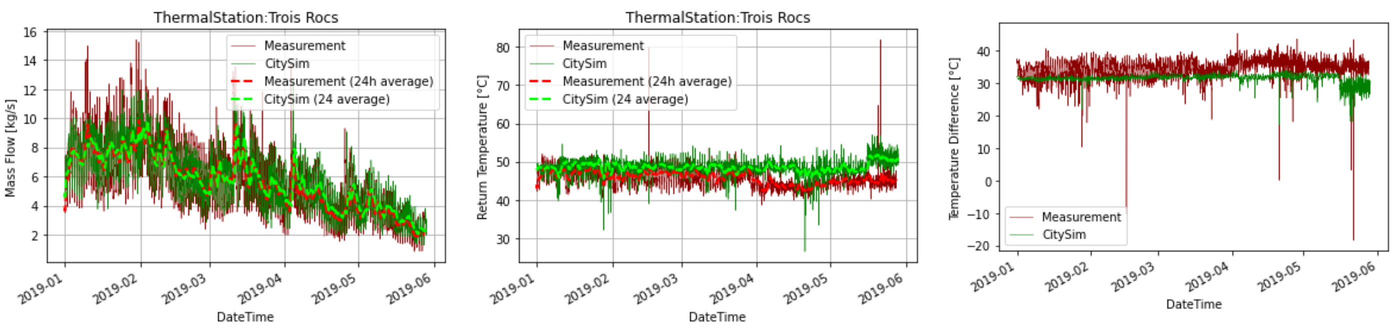


Figure 4.7: *The comparison between the CitySim simulation and the measurement at the Trois Rocs thermal station for the mass flow (left), the entering temperature (middle) and temperature difference between the entering and exiting temperature (right).*

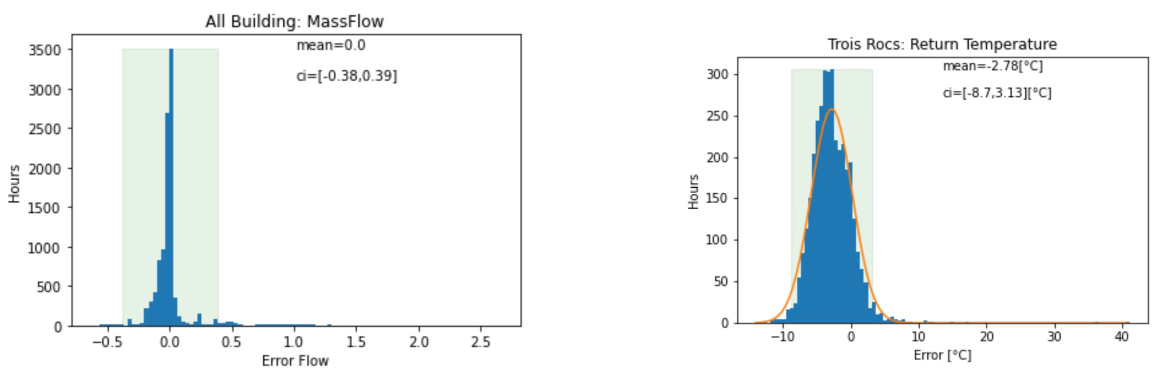


Figure 4.8: *Distribution of the absolute errors between the CitySim simulation and the measurement on the mass flow (left) and the entering temperature (right) at the Trois Rocs thermal station, with the 95% confidence interval. Considering the period going from the 1st of January to the 28th of May 2019.*

The differences observed in the Fig.4.7 are hardly visible due to the oscillations. Nevertheless, it already demonstrates that the model is in the correct range for both parameters. Moreover, the daily confirms this first impression and indicates that the trend is correct. One can notice that the oscillations for both plots, and especially the one on the left-hand side are bigger for the measurement than the simulation. As explained previously, it is simply due to the fact that the simulation always find a stationary solution at each time step while the energy conversion has continuous changes of heat demand which destabilises it and move it further away from its stationary solution.

Focusing on the return temperature, even though the trends are very similar, the relative error between the measurement and simulation is on average bigger. The relative error for the return temperature is 5.6% while the one from the mass flow is 2.3%. The relative error on the daily averages is further decreased to respectively 4.5% and 0.9%. This might be due to the fact that the thermal losses are not computed correctly. In addition, two peaks are visible for the measurement. During these time steps, the return temperature is reaching the supply one, meaning that no building is consuming. It should be checked with the operators, but probably, during these time steps, the district heating was under maintenance. These events are of course not included in CitySim.

The distribution of the errors in Fig.4.8 offers a different analysis of the differences between simulation and measurement. The error distribution is centred close to zero for the mass flow and slightly shifted for the return temperature. This shift could be corrected simply by changing the overall temperature difference at the substations. The distribution gives also the confidence interval of 95% of each variable. The confidence interval is of the order of 50% for the mass flow and 10% for the return temperature. Thus, the uncertainty of a mass flow simulated at each time step is non-negligible. However, the confidence intervals are reduced when considering the daily averages to 15% and 5%.

Concerning the power delivered by the heating station, the Fig.4.9 is very similar to the one with the mass flow. The differences are certainly due to latency of the system, as it is derived from the other.

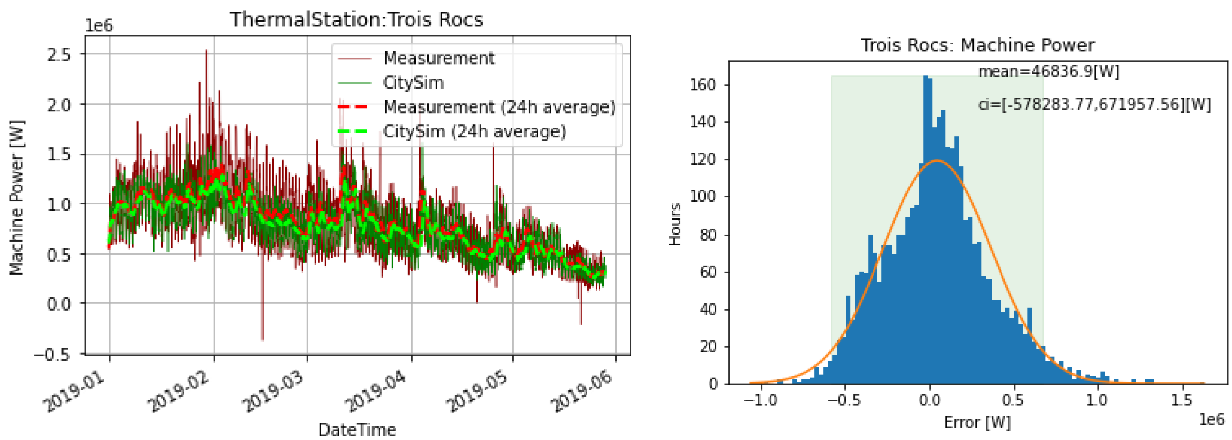


Figure 4.9: *The evolution and the distribution of the error of the thermal power delivered at the Trois Rocs thermal station.*

In this figure, the amplitude of the measurement is still higher as it is coupled with the mass flow. The answer for this is therefore identical to the one provided for the mass flow. Nevertheless, the daily averages are once again very close to each other, giving a mean relative error of 4.6%. The errors of both variables are accumulated. The mean of the distribution is almost centred on zero as the previous mean distribution of the mass flow and the return temperature that respectively decrease and increase the thermal power delivered. In the end, they compensate each other. The confidence interval is very large, since it is of the order of 50%.

Moving to the evaluation of the substations, only few typical substations are displayed, showing the different errors found through this study. In addition, the time period for the comparison has also been reduced in order to see more clearly the differences. Indeed, the substations, as opposed to the heating station, are varying much faster following directly the heat demand. The period selected for the study corresponds to the period with the higher power consumed. It starts on the 24th of January and ends on the 7th of February 2019. Choosing the period with the highest consumption allows to have more substations to compare the simulation with.

The first substation to be studied is the number 860. This substation is situated at the opposite side of the network and provides the heat to one of the biggest consumer of the network as it is possible to notice with the Machine Power in Fig.4.10. The results regarding the heat provided by the network is excellent and confirm the results obtained on the case study on Broc. Concerning the mass flow, it is overestimated since the temperature difference is at 40°C instead of 30°C as assumed for every substation. Therefore, it implies a higher mass flow as the heat demand is still fulfilled.

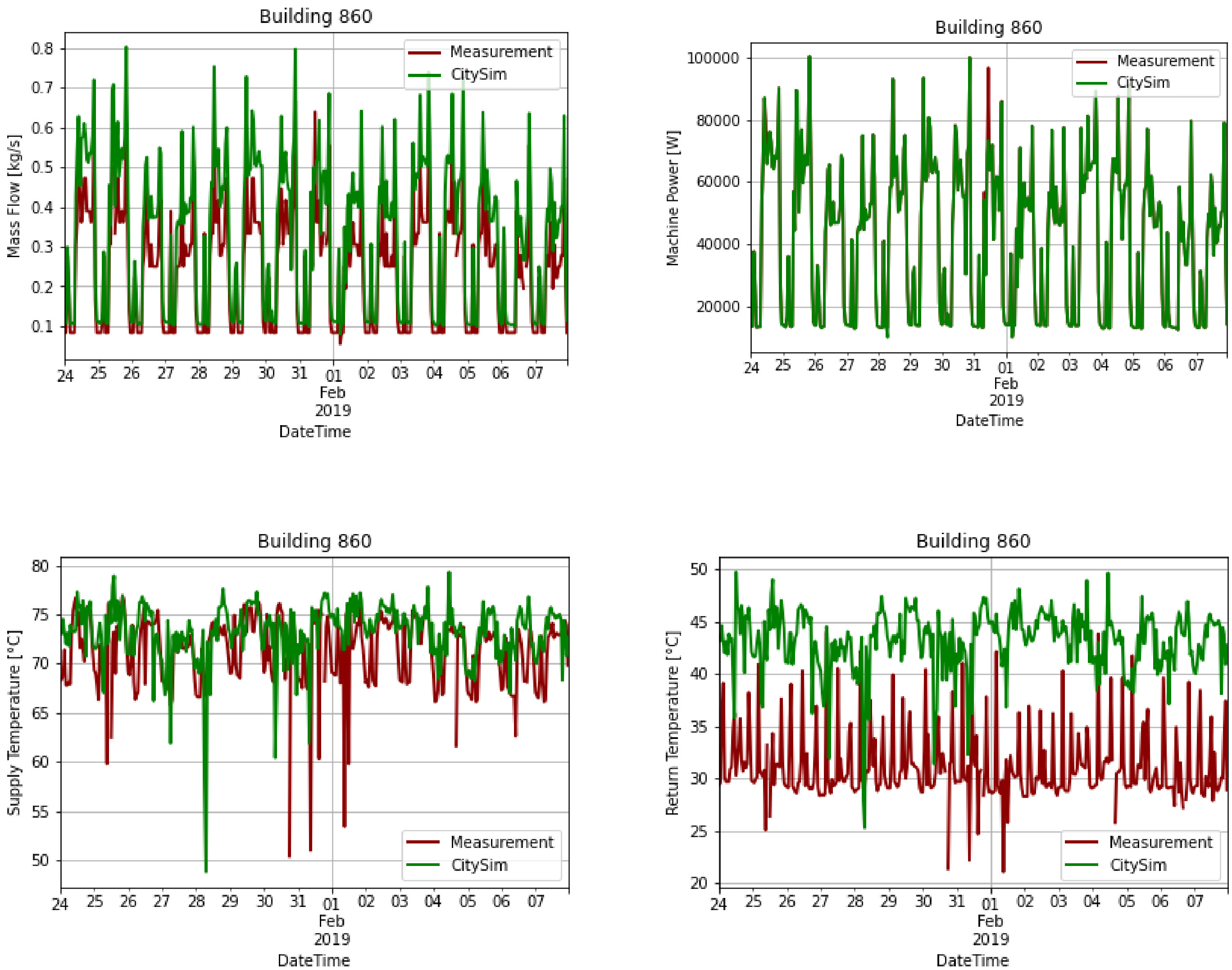


Figure 4.10: *Comparison between the results of CitySim and the measured data at the substation 860.*

A higher mass flow changes the thermal dynamic in the pipe, which creates slight changes in the estimation of the supply temperature. Finally, the error between the simulation and the measurement is the biggest at the return temperature since it is computed on the basis of the supply temperature and the heat demand wanted at the substation, which in the end comes to the hypothesis of constant $\Delta T$ at the substations. It is interesting to note that in reality, the temperature difference is not constant through time. Hence, the hypothesis done is very restrictive. By discussing with the operators of Verbier, it has been discovered that the mass flow at the substation was in reality established using the entering temperature of the secondary network. Unfortunately, no data were available anymore on the period of interest. As a further improvement in the CitySim, it could be thought to change the computations of the desired mass flow in order to take into account the secondary network.

The overall distribution of the absolute errors for the buildings are given in the Fig.4.11. The absolute error is given as the $data_{measured} - data_{simulated}$. Considering every building, the precision between the different benchmark follows what was observed in Fig.4.10. The error on the heat demand is very small even though the confidence interval is of the order of 10kW that is highly perturbed by localized non converged steps. The error gets bigger for the mass flow, but it is still showing acceptable results with a confidence interval lower than 0.5 kg/s. Going to the temperatures, the distributions indicate two types of errors when looking at the supply temperatures. The small errors are due to the approximation of constant temperature difference at the substations, which approximates the mass flow and changes the thermal exchanges between the pipe and the fluid.

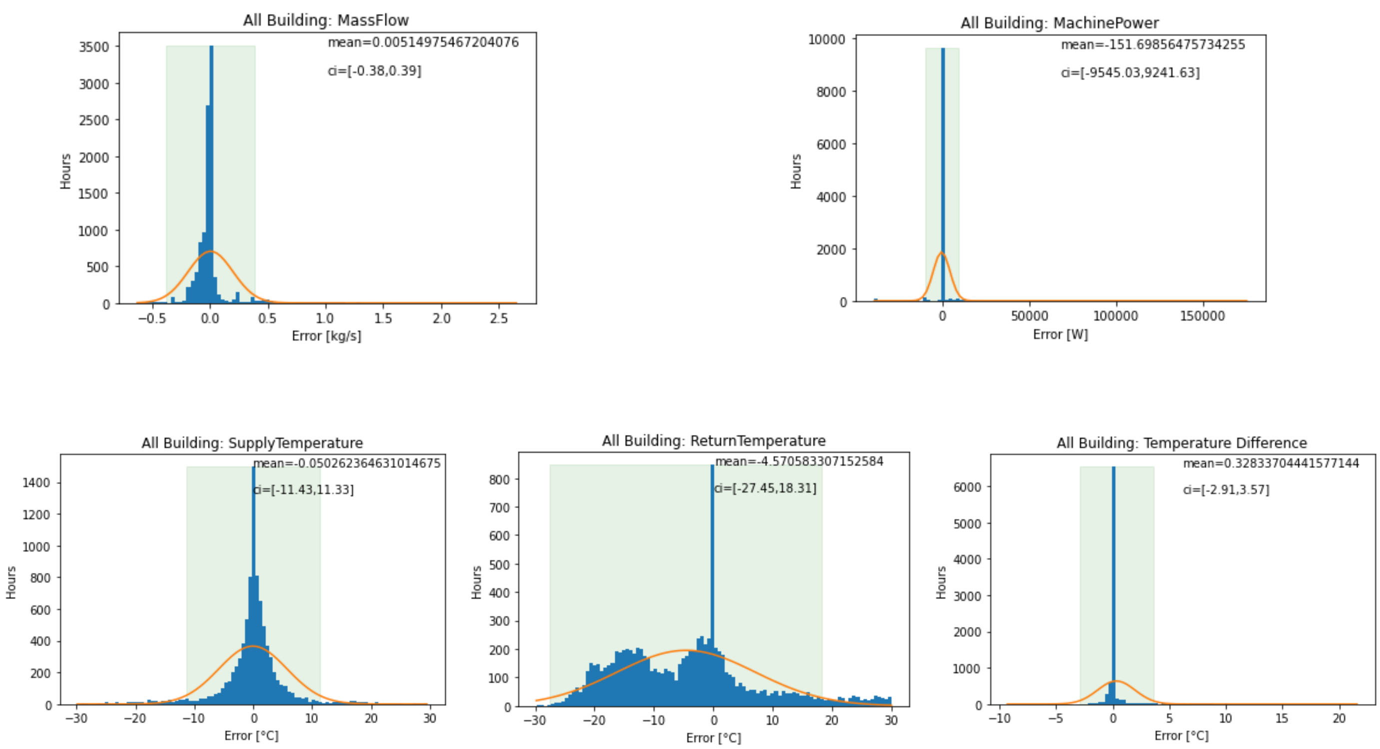


Figure 4.11: *Distribution of the absolute errors between the CitySim simulation and the measurement on the overall buildings with the 95% confidence interval for the benchmarks of the substation and the errors on the target temperature of $\Delta T = 30°C$ at every substation. Considering the period going from the 1st of January to the 28th of May 2019.*

The big errors are more difficult to explain. Those types of errors are appearing in substations such as the one numbered 2704. In this substation, the heat exchanger is totally shut down several times a day. Therefore, the mass flow traversing the heat exchanger is almost zero. The pipe arriving at the substation becomes a 'dead branch'. In the simulations, it is never the case, as a minimum opening of the valve is set in order to avoid infinite pressure difference. The mass flow is usually of the order of $10^{-4}$ which is negligible compared to the usual mass flows that are circulating in the network. As a consequence, in the simulations, the temperature is of course dropping at the ground temperature as the stationary solution is found. Concerning the measurements, the measures are staying at the same range of temperatures. One could think about this is caused by internal convection movements inside the pipe allowing some transfer of heat, but it is not probable since according to the operators of the network of Verbier, the dead branches have a higher static pressure in comparison to the rest of the network. Thus, the main network that is still flowing is only inducing micro convection. An explanation for this would simply be that the temperature sensors are not located at the same place as the flow meter. Nevertheless, this was not confirmed by the operators and hence it remains an open question. These perturbations perturb the confidence interval of the supply temperature. Removing the errors when the power is going to zero, the confidence interval goes within a range of [-11.4, 11.33]°C.

Coming back to the Fig.4.11, the distribution of the return temperatures is spread. It is due to the fact that the heat exchangers of the network are in reality not at a fixed $\Delta T$. One solution would be to simply add, as an imposed for each time step, a $\Delta T$ as it is done for the heat demand, but it is not the purpose of the model. The other solution proposed is to simulate the secondary network in order to establish the return temperature of the network. Considering the last plot, the constraint at the substation is well followed, meaning that the problem is coming from the computation of the desired mass flow. In fact, the model is converging on the value it has been assigned to. This means that given a new rule in order to set the desired mass flow such as the one mentioned previously, the computational framework is likely to converge on the correct desired mass flow.

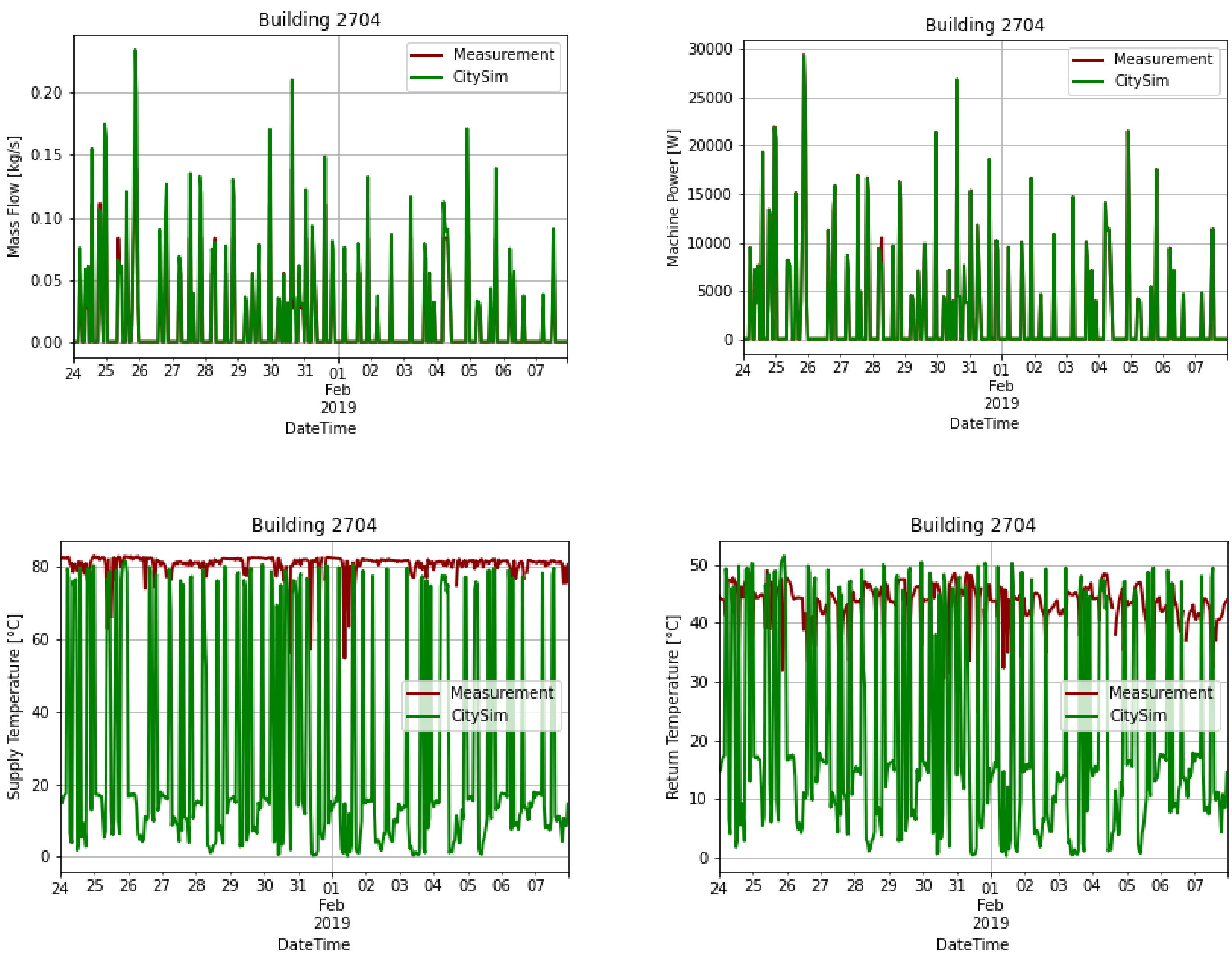


Figure 4.12: *Comparison between the results of CitySim with the measured data at the substation 2704.*

In the end, given the production of the heating station and the total consumption of every building, it is possible to deduce the heat losses through the network. In fact, in order to close the energy conservation, the total energy produced is equal to the total energy consumed plus the total energy lost. The latter corresponds to the heat that went to the ground. The operators are thus interested in minimizing in order to reduce the cost linked to the fuel consumption. Therefore, concerning CitySim, it is primordial to evaluate this quantity correctly. The Fig.4.13 shows the evolution of the measured and simulated thermal losses in the network during the period starting on the 1st of January to the 28th of May.

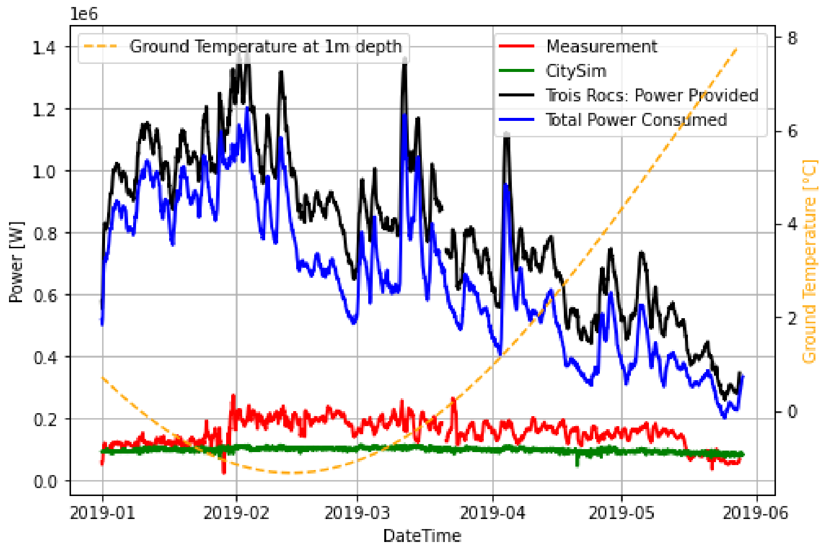


Figure 4.13: *The comparison between the measured and simulated thermal losses of the network of Verbier along the total power provided by the heating station, the total power consumed by the buildings and the estimated ground temperature at a depth of 1m.*

The differences observed in the Fig.4.13 might be due to many reasons. For example, the pipes have been buried all at the same depth of 1m but in the network the depth are varying as well as the soil conductivity. Another uncertainty is given on the insulation of the pipe. Of course, the model and the nominal diameter of each were known, but unfortunately the insulation of those pipes also depends on the year they were produced. This is not supposed to play an important role, but still contributes to possible mistakes. Nevertheless, as the measured thermal losses seems to change with respect to the change of the soil temperature, it means that the pipes are more sensitive to soil conditions. Therefore, either a higher soil conductivity or shallower buried pipes or smaller insulation thicknesses might correct these differences. This thermal loss in the network of Verbier are of the order of 10% of the total heat injected by the heating station of the Trois Rocs.

### Validation of the MCR

This paragraph aims to validate the MCR implementation, as it was not possible with the network of Verbier. In order to test the MCR, the nominal power of the Trois Rocs became 1.2 MW imposing the Trois Rocs to saturate and Mondzeu has been decreased to 400 kW. For Mondzeu, there have been defined 4 stages in order to see the changes of stage during the simulation. They are equally distributed between 0 and the nominal power of the heating station. The latency of the slave was set at 1 hour. It was recommended when discussing with RWB a company of district heating simulation about the implementation of this new class. In fact, it takes time for a heating station to reach its optimal mode. Therefore, it is inefficient to switch on and off successively the energy conversion system [8]. The exiting temperature setpoints have also been modified. For the Trois Rocs and Mondzeu, they are exactly the same and constant at 80°C. The Fig.4.14 is used in order to validate the model implemented.

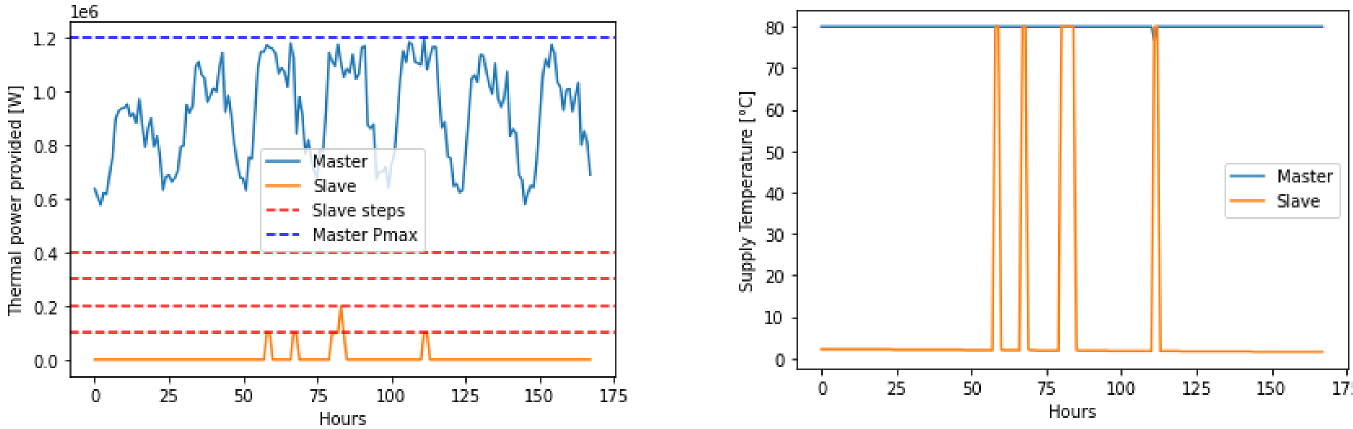


Figure 4.14: *Evolution of the thermal power (left) and exiting temperatures (right) for the two heating stations, with the hour 1 corresponding to the 1st of January 2019.*

The left-hand side of Fig.4.14 shows that the evolution of the slave heating station is done by step if the master heating station gets saturated. It is also possible to see the latency of 1 hour imposed to the slave. Finally, the right-hand side of the Fig.4.14 checks whether the supply temperature setpoints are well respected. Interestingly at one point the supply temperature of the master heating station is decreasing meaning that it was saturated. This matches with the constraint that the slave heating station can only jump from one stage at each time step.

The Fig.4.15 allows to visualise the MCR in the network.

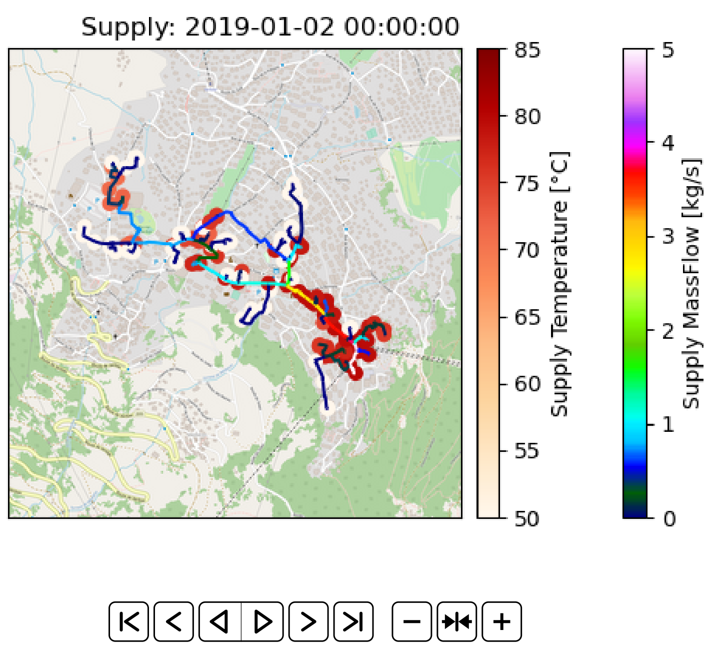


Figure 4.15: *GIF of the evolution of the supply temperature and the mass flow in the network of Verbier following the MCR implemented in CitySim.*

The heating station of Mondzeu, situated under the loop of the network see on Fig.4.4, works on the 3rd of January at 8-9 a.m. and 6-7 p.m. corresponding respectively at the first and second peak on Fig.4.14.

### Conclusion

As a conclusion, CitySim allows simulating accurately the trends of the heating station. However, when the comparison is done on an hourly basis, the system does not follow the oscillation observed in the Fig.4.7. On the same figure, the positive point is that the temperature difference at the substations follows well the target temperature difference of 30°C. Hence, it means that if a new rule is implemented in a future work, it is likely that the software converges on the correct solution. Therefore, a very simple way to improve the results would have been to get the difference temperatures for each substation at every time steps in order to get accurate desired mass flows, but it is not a likely solution since it is not convenient to get all these data. From the discussion with the operators of the network of Verbier, they manage the opening of the valves at the substations depending on the supply temperature desired on the secondary network. Consequently, as a further improvement, it could have been interesting to get the target temperature entering the building and establish the opening according to it.

CHAPTER 5

# CASE STUDY OF YVERDON: APPLICATION TO A LOW ENTHALPY DISTRICT HEATING NETWORK

## 5.1 Introduction

This chapter aims to study a district heating network of the last generation. The objective is to validate the software on low temperature district heating network at first.

Then, studies have been driven on the comparison of different connection scenarios. The key performance indicators used in order to compare the different scenarios are the thermal losses in the network and the electric consumption of the pump and compressors. These KPIs were chosen as they are directly linked to the operating costs of the system. They are consequently of primal importance for the operators of this DHN.

This analysis has thus been useful for the city in Yverdon in order to evaluate the potential of solar heating in the future extensions of their DHN and to limit their expenses.

### 5.1.1 Historical details about district heating networks

Through the years and generations, the supply temperatures in the district heating networks tend to decrease. In fact, the first generation of district heating networks appeared in the late ninetieth century. At that time, the idea of district heating appeared in order to solve problems of individual heating systems inefficiencies and waste treatments. The centralised heat was generated by burning coal and urban wastes. The supply temperature was around 200°C and the water was carried out in the form of steam. It was first implemented in Manhattan and it is still in function nowadays. Nevertheless, this generation of DHNs has many drawbacks. The steam system requires large pipes and therefore makes it expensive to build and maintain.

The second generation of district heating networks appeared with the development of new pumping technology in the 1930's. It allowed then to use pressurised water as energy carrier through the system. It allowed improving the energy efficiency as the supply temperature was below 100°C and was easier to build and maintain.

Fifty years later, a third generation of district heating networks started to be implemented lowering, even more, the supply temperature around 90 to 70°C. The district heating of Verbier and Broc that were studied in the previous chapter are from this generation. It is for now the most developed district heating network in the world. With the arrival of the third generation, new fuels have been used in order to heat up the fluid such as biomass and solar thermal.

In the recent years, the many concerns about the environment and the electrification of our energy due to the development of renewable energies have motivated the implementation of the fourth generation of DHNs. This new type inserts itself in the concept of smart cities that are currently developed in scandinavian countries. The supply temperature of this DHN is below 60°C changing the way the heat is exchanged at the substations. In the previous generation, there was simply a heat exchanger at the substation as the supply network was hotter than the temperature needed by the building. The fourth generation needs heat pumps as connecting elements between the primary and secondary network in order to heat the hot source (i.e. the Domestic Hot Water) with the cold source (i.e. the supply network). Decreasing the supply temperature allows to reduce the thermal losses in the ground to almost zero and to recycle heat from low temperature sources and integrate renewable heat sources such as solar and geothermal heat. As an example, the case study of Yverdon that has been driven uses the heat from a wastewater treatment plant. [7]

### 5.1.2 Presentation of the case study

As previously mentioned, the low temperature DHN of Yverdon is studied. This DHN is currently developed by the city of Yverdon-Les-Bains and lies in the center of the city on the shore of the lake of Neuchâtel. This district is illustrated in the Fig. 5.1 with the different forecast extensions. The municipality wants to develop in the following years an eco-district named "Gare Lac" in which the DHN aims to supply their heating demand. This eco-district is represented by the buildings in yellow and green on the Fig. 5.1. The project is rather new as it started only a year ago and is supplying already six buildings. The DHN is for now using the wastewater treatment plant in order to supply the heat demand of its consumers. With the development of the eco-district and the connection of new municipal buildings such as the restaurant of the tennis field visible in purple on the Fig.5.1, they need additional heat sources. They chose to implement solar panels on the new buildings rooftop as their objective is to rely only on renewable energies. These solar panels are forecast to be implemented only on future buildings which are characterised with the name 'Block' in the Fig.5.1. It has been assumed that 50% of the roof area of each of these buildings will be covered with solar panels.

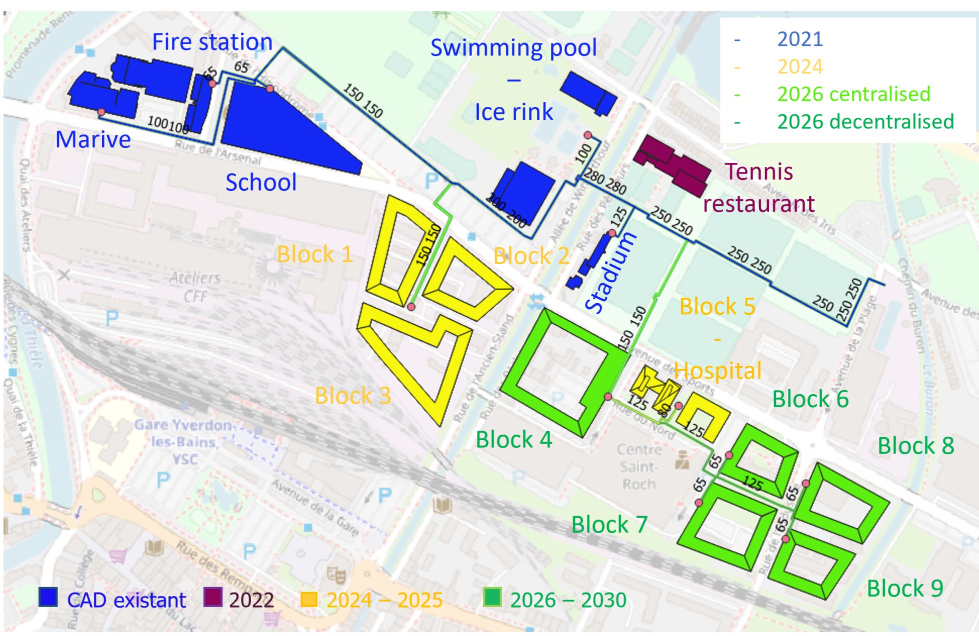


Figure 5.1: *QGIS visualisation of the district heating network of Yverdon. The different colors represent the different extensions that are planned while the numbers appearing close to the DHN correspond to the nominal diameter of the pipes.*

In comparison with the previous case study, simulations are done on buildings that are not even existing yet. Hence, without the heat demand, the 3D models of the buildings were needed. Thanks to Pierre Van Brockhoven that did his master thesis at kaemco, the geometry, wall compositions, and all the information needed by CitySim in order to compute the energy demand of every building were obtained. The 2D projection of his work is visible on the QGIS visualisation of the DHN of Yverdon [21]. He also established the brand and model of the thermal panels considered.

The occupancy profiles were also set during his work. They are very important since the DHN is connected to many different types of facilities. The building for example at the extrema of the network is an auditorium while the two buildings in blue nearby are respectively a fire station and a school. The other three edifices already connected are the ice rink and the swimming people on the same heat pump and a stadium. For future extensions, the eco-district is supposed to be residential. The occupancy profiles given by the SIA norm show very distinct profiles which induces very different heating demand profiles.

The information on the network such as the nominal diameter of the pipes or the nominal power of each substation were acquired thanks to the report of Planair that made estimations of the dimensions of the different elements in 2018 [24]. The nominal diameter of the pipes is essential for the simulation, since the constructor has defined insulation thicknesses and diameters for each size. Following the Planair report, the model Brugg Premant insolation 1 has been chosen for the pipes [25]. The route of the network was determined according to the planning of the city of Yverdon. In the end, the data concerning the network were stored on a PostgreSQL database under the following form.

| | obj_id bigint | dn_descrip character varying | length double precision | geometry geometry | altitude double precision | alt_start double precision | alt_end double precision | start_point_id integer | end_point_id integer |
|---|---|---|---|---|---|---|---|---|---|
| 1 | 1001 | 250 | 86.442 | 010500008001000... | 500 | 500 | 500 | 0 | 11 |
| 2 | 2001 | 250 | 56.774 | 010500008001000... | 500 | 500 | 500 | 1 | 0 |
| 3 | 4001 | 250 | 175.566 | 010500008001000... | 500 | 500 | 500 | 2 | 1 |

Figure 5.2: *Partial content of the table pipe in the PostgreSQL database describing the network of Yverdon.*

In Fig.5.2, obj_id gives a unique id for each pipe, dn_descrip represents the DN of each pipe, the geometry is given under the hexadecimal form and is useful for the establishment of singular pressure losses, the altitudes, and the id of the points that are respectively at both sides of each pipe. The table for the points has also been uploaded to this database. It is composed of four columns. The location, altitude, id of each point are stored. In addition, the home_id corresponds to the id of the building the point is connected to. By convention, the NaN means that the point is not connected to any buildings. This table is displayed in the appendices.

## 5.2 Implementation of the connecting elements

CitySim was at the beginning of this thesis, not designed for the simulation of low temperature district heating networks. In fact, the only connecting elements implemented were heat exchangers, represented by the class Substation and ProsumerSubstation which enable the injection of solar thermal in the network. Since the temperatures of supply of the primary network, around 15°C for Yverdon, are below the one required for the secondary network, around 60°C, the heat supply is not possible with a simple heat exchanger. Usually, in low temperature district heating networks, heat pumps are therefore implemented in place of the substation.

### 5.2.1 The Substation Heat Pump

The heat pumps are parts of the sustainable energy conversion systems. They are commonly used in the household sector for heating or cooling purposes.

A heat pump is mainly composed of an evaporator, a condenser, a compressor, and a valve as it is shown in the Fig.5.3 on the right-hand side. This device allows warming the building by transferring the energy from a cooler source (evaporator) to a hotter one (condenser). This transfer of energy is made possible by compressing and expanding the working fluid that travels in between the two heat exchangers. Indeed at the evaporator, which is in our case study the part in contact with the primary network, is at low pressure and therefore at low temperature. The fluid gets heated at the evaporator and then is compressed in order to reach higher temperatures and switch from a fluid to a gas state.

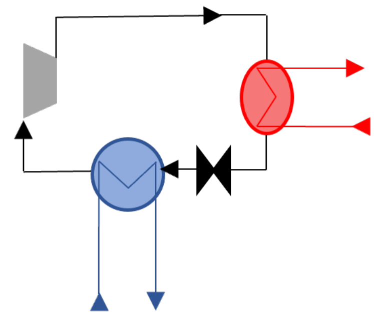

Figure 5.3: *The schematics of a heat pump.*

At higher pressure, this working fluid releases its energy by condensing at the second heat exchanger in contact in our case with the secondary network at a higher temperature. Finally, the fluid goes through a valve and reaches its starting point at a low pressure ready to start another cycle. The advantage of this technology is that usually, the cold source is a free energy which can be the air or geothermal sources meaning that only the electricity needed by the compressor has to be paid. The efficiency of a heat pump is hence described by its Coefficient Of Performance (COP) which can be expressed as the following,

$$COP = \frac{\dot{Q}_{cond}}{\dot{E}_{compr}} = \eta \frac{T_h}{T_h - T_c} \tag{5.1}$$

where $\eta$ is the technical efficiency while the second term with the temperature of the hot source $T_h$ and cold source $T_c$ corresponds to the Carnot efficiency. This COP varies depending on the various working fluid and types of heat pumps. One of the most efficient heat pumps is the water source heat pump since water has a better heat transfer compared to air. In addition to very high efficiencies, the heat pumps also allow moving towards an electrification of our heating supply which helps the integration of renewable energies such as PV panels or windmills. Finally, the heat pumps are not only used for heating purposes but also for cooling. We just have to reverse the flow of the working fluid and the cold and hot sources are switched. This property could be even more useful in Switzerland since deadly heat waves are expected to happen more frequently in the next summers due to climate change. For these reasons, the heat pumps are an interesting solution as connecting elements in district heating networks.

In CitySim, a new class SubstationHeatPump has been created in order to simulate the low temperature DHN. This class is a subclass of SubstationProsumer with an attribute HeatPump as it combines properties of both. Being the subclass of SubstationProsumer, it inherits from the property solar thermal injection in the network. This property will be particularly useful and discussed in the section 5.5. The SubstationHeatPump also work in two different modes as it can inject some energy in the network if it has solar panels and its demand is entirely fulfilled and it can be as well a consumer if the building still has some heating demand. According to the formula (2.2), the solar thermal efficiency increases with the reduction of the temperature difference between the external temperature and the temperature of the fluid injected. Therefore, the solar energy is injected directly with a simple heat exchanger without interacting with the heat pump. It allows lowering the target temperature of the panels. The Producer mode is thus identical to the one from the ProsumerSubstation. However, when it is in consumer mode, the heat exchange has to be carried out by the heat pump.

In the code, the heat pump is considered as a black box ignoring the hydraulics of the working fluid. Therefore as the heat demand is known and the technical efficiency is given as an input by the user, the power extracted from the network is simply given by the following expression.

$$\dot{Q}_{DHN} = \dot{Q}_{demand} - \dot{E} = (\eta \frac{T_h}{T_h - T_c} - 1)\dot{E} \tag{5.2}$$

One can notice with the equation (5.2) that the thermal power extracted from the primary network is depending on the supply and return temperatures of the network. Therefore, even in consumer mode, the desired mass flow has to be updated after each thermal equilibrium. In this thesis, a simplification is made in the computations of the thermal power extracted. The temperature $T_c$ is supposed as constant. This assumes that we have basically an infinitely large cool source reservoir or an infinite mass flow. It is of course not the case since we are considering as we will see it later a design temperature difference of 5°C at the evaporator.

### 5.2.2 The substation 2-stages Heat Pump

Another connecting element has been implemented in the code which is the 2-stages heat pump. The motivation to implement this new connecting element is coming from the fact that the heating needs nowadays for buildings are at two different temperatures. Indeed, the Domestic Hot Water needs to be above 60°C in order to avoid health risks caused by legionella bacteria growth as the hot water is stored in a heat tank. Concerning space heating, the radiators required temperatures around 70°C however with the advent of floor heating in modern buildings, it allowed to lower the temperatures to 30-40°C [23]. From the point of view of the performance of the heat pump, it is therefore convenient to use multi-temperatures heat pumps since the COP is divided by the difference of temperature between the cold and the hot sources. Moreover, the multi-stages heat pumps are more efficient because they use different working fluids for each stage, that are more adapted to work in specific temperature ranges.

This differentiation of the working fluid induces higher technical efficiencies for each stage of the heat pump. Many different multi-temperatures heat pumps are currently different developed mostly for industrial use as it is well described in the literature review [22]. In the computational framework, a cascade heat pump has been implemented since it is already used for the separation of the space heating and domestic water heating processes. The schematic of how was imagined the multi-stages heat pump for CitySim, is shown on the Fig.5.4. It is mainly composed of two evaporators, one condenser, one heat exchanger, two compressors, and two valves. The blue part represents the evaporator exchanging heat with the primary network while the yellow and red parts represent respectively the condenser supplying the space heating and DHW needs.

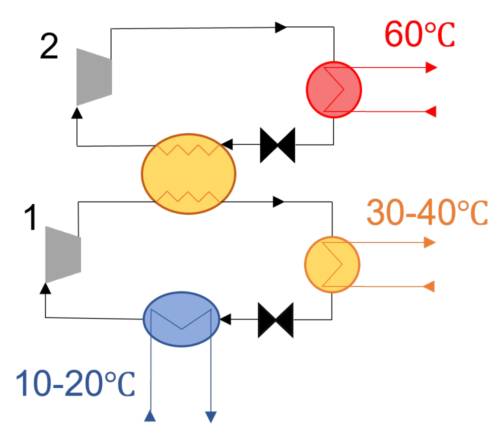


Figure 5.4: *The schematics of the two stages heat pump implemented in CitySim.*

In CitySim, the multi-stages heat pumps appear under the class name SubstationHeatPump2stages which is a subclass of SubstationHeatpump and Substation. As for the substation heat pump, the 2-stages heat pump is considered as two black boxes having energy exchanges between them. Consequently, for each stage, there is a COP and a technical efficiency. Nevertheless, the algorithms required in order to compute the exiting temperature of a substation 2-stages and the work consumed by the compressors were a bit more complex than the ones for the substation heat pumps.

Regarding the algorithm to compute the electricity consumption of the heat pump given the thermal power that has to be provided, it has first been established that the energy conversion system had to fulfill the DHW demand in priority. Indeed, the tank where is stored the DHW has to be above 60° if we want to avoid issues linked to the legionella. Therefore as it is represented in the Fig. 5.4, the heat exchanger in between the two heat pumps is placed before the heat exchanger supplying the space heating. The model computes the electricity by considering the total thermal power available. Hence, if the total available thermal power is bigger than the DHW demand, it computes the electricity necessary to fulfill this demand. Then, the algorithm looks if the DHN can also satisfy the space heating needs or if it just has to give what's remaining. Finally, if the available thermal power is smaller than the DHW demand, it gives the electricity that is consumed in order to all the available heat. As it is shown in the algorithm 6, one has to be careful while computing the electricity needed for the supply of the DHW needs because the work is split on the two compressors.

**Algorithm 6:** *Establishment of the electric consumption of both compressors*

**Function** $getWork(\dot{Q}^{th}_{tot}, T_{LT})$:
  $T'_{MT} \leftarrow T_{MT} + \Delta T_{design}$
  **if** $\dot{Q}^{th}_{tot} > \dot{Q}^{Needed}_{DHW}$ **then**
    //Priority to the DHW
    $\dot{E}_{DHW} \leftarrow \frac{\dot{Q}^{Needed}_{DHW}}{\eta_{DHW} \cdot COP_{DHW}(T'_{MT}, T_{HT})}$
    $\dot{E}_{HSforDHW} \leftarrow \frac{\dot{Q}^{Needed}_{DHW} - \dot{E}_{DHW}}{\eta_{HS} \cdot COP_{HS}(T_{LT}, T'_{MT})}$
    **if** $\dot{Q}_{th,tot} > \dot{Q}^{Needed}_{DHW} + \dot{Q}^{Needed}_{HS}$ **then**
      // There is enough thermal power to supply all needs
      $\dot{E}_{HS} \leftarrow \frac{\dot{Q}^{Needed}_{HS}}{\eta_{HS} \cdot COP_{HS}(T_{LT}, T'_{MT})}$
    **else**
      // Give the remaining heat to the space heating
      $\dot{E}_{HS} \leftarrow \frac{\dot{Q}^{th}_{tot} - \dot{Q}^{Needed}_{DHW}}{\eta_{HS} \cdot COP_{HS}(T_{LT}, T'_{MT})}$
    **end**
  **else**
    // Give everyting to the DHW heating
    $\dot{E}_{DHW} \leftarrow \frac{\dot{Q}^{th}_{tot}}{\eta_{DHW} \cdot COP_{DHW}(T'_{MT}, T_{HT})}$
    $\dot{E}_{HSforDHW} \leftarrow \frac{\dot{Q}^{th}_{tot} - \dot{E}_{DHW}}{\eta_{HS} \cdot COP_{HS}(T_{LT}, T'_{MT})}$
  **end**
  **return** $\dot{E}_{DHW}, \dot{E}_{HS} + \dot{E}_{HSforDHW}$
**End Function**

Concerning the establishment of the exiting temperature at the evaporator, the computations are inspired by what was done for the substation. The only thing that changes is the previous establishment of the electricity required in order to obtain in the end the power, $\dot{Q}^{th}_{exch}$, exchanged at the evaporator. There is also an additional sizing constraint with respect to the substation. In fact, the electricity is also constrained with the function $getWorkAvailable()$. Finally, as for the substation, the thermal power exchanged is set to 0 if the flow goes backward. However, in future implementations, it could be interesting to set a negative power since it is also possible to cool down the building thanks to heat pumps. It would mean then that the flow has to go backward and we would then go back to the case of a prosumer.

**Algorithm 7:** *Determines the temperature exiting a substation 2-stages heat pump.*

**Function** $computeHeatExchanged(C_p, \rho, T_{in}, \dot{M}_{prim}, \Delta P_{prim})$**:**
    **if** $\dot{M}_{prim} > 0$ **then**
        // Get the electric consumption needed for both compressors
        $\dot{E}^{Needed}_{DHW}, \dot{E}^{Needed}_{HS} \leftarrow getWork(\dot{Q}^{Needed}_{tot}, T_{in})$
        $\dot{E}_{DHW}, \dot{E}_{Hs} \leftarrow getWorkAvailable(\dot{E}^{Needed}_{DHW}, \dot{E}^{Needed}_{HS}, \dot{E}^{Max}_{DHW}, \dot{E}^{Max}_{HS})$
        $\dot{Q}^{th}_{tot} \leftarrow \sum_{i=DHW,HS} \dot{E}_i \eta_i COP_i$
        // Compute the heat exchanged with the primary network
        $\dot{Q}^{th}_{exch} \leftarrow \dot{Q}^{th}_{tot} - \dot{E}_{DHW} - \dot{E}_{Hs}$
        // Get the electric consumption of both compressors at $\dot{Q}^{th}_{design}$
        $\dot{E}^{design}_{DHW}, \dot{E}^{design}_{HS} \leftarrow getWork(\dot{Q}^{th}_{design}, T_{in})$
        **if** $\dot{Q}^{th}_{exch} > \dot{Q}^{th}_{design} - \dot{E}^{design}_{DHW} - \dot{E}^{design}_{HS}$ **then**
            $\dot{Q}^{th}_{exch} \leftarrow \dot{Q}^{th}_{design} - \dot{E}^{design}_{DHW} - \dot{E}^{design}_{HS}$
        **end**
    **else**
        // The space cooling has not been implemented yet
        $\dot{Q}^{th}_{exch} \leftarrow 0$
    **end**
    **Result** $T_{out} \leftarrow computeOutputTemperature(T_{in}, \dot{Q}^{th}_{exch}, \dot{M}_{prim}, \Delta P_{prim}, \rho, C_p)$
**End Function**

The required parameters for the simulation are the following: the entering temperatures for the space heating and DHW, the size of the compressors, the technical efficiencies of each "sub" heat pump, the id of the node it is linked to, the design thermal power and the design temperature difference. For now, the SubsationHeatPump2stages have two sizing constraints that are dependent. One on the size of each compressor and one on the design thermal power. It has not been reduced since, for the following study on Yverdon, the constraint of the thermal power was given even though the size of heat pumps are usually given by the size of their compressor.

## 5.3 Validation of the CitySim tool on the case study of Yverdon

The validation of the software is carried out with the case study of Yverdon presented in section 5.1.2. As previously mentioned, the network is rather new. Therefore, the monitoring of this network did not allow a validation of CitySim through data analysis as it was the case for Verbier. Some data are missing and the network is frequently stopped for repairs and tests which makes the few data available hard to compare. Consequently, the validation is based more on plausibility.

### 5.3.1 Hypothesis and benchmark

Few hypotheses were made based on the Planair report in order to conduct this validation. They are displayed in the table 5.1.

| | 2021 | 2022 | 2024 | 2026 |
|---|---|---|---|---|
| Thermal Power STEP [kW] | 1920 | 1920 | 1920 | 2760 |
| Pipes Model | Brug Premant Isolation 1 | | | |
| Pipes depth [m] | 1 | | | |
| Inter pipe distance [m] | 0.66 | | | |
| $\Delta T_{design}^{evap}$ [°C] | 5 | | | |
| $\eta_{HP}$ [%] | 70.6 | | | |
| $T_{cond}$ [°C] | 62 | | | |
| soil Conductivity [W/mK] | 0.5 | | | |

Table 5.1: *Hypothesis considered for the simulation on the DHN of Yverdon. [24]*

One can notice that the $\Delta T_{design}^{evap}$ is significantly smaller than the ones taken in the case study of Verbier around 30°C. This is simply due to the fact that the design temperature difference at the heat pumps is limited is since the water does not have to freeze in the pipes. In the case study of Yverdon, the Planair report states that the limit temperature that does not have to overcome in the entire network is 4°C. A margin is taken since a change of state in the DHN would cause serious damages. This smaller $\Delta T_{design}^{evap}$ induces higher mass flows in low temperature DHN as it will be observed in the section 5.3.2.

In addition to the hypothesis set in the table 5.1, the pressure difference and the efficiency of the pump at the heat exchanger called STAP in the STEP are simply considered as linear by parts. Regarding, the idea behind this dependency is coming from the fact that the pressure losses in the pipes are increasing with the mass flow. Hence, the pressure difference at the STAP has to increase in order to overcome all these pressure losses. The resulting characteristic curves are shown in the Fig. 5.5.

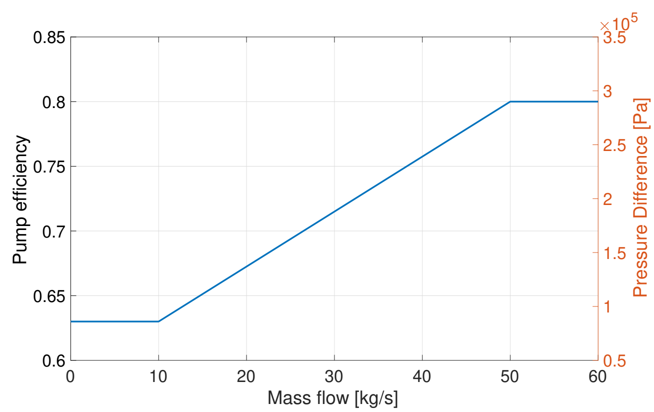


Figure 5.5: *The characteristic curve of the pump at the heat exchanger STAP of the STEP. [24]*

This method of setting the pressure difference was already existing in CitySim and it just has to be extended for the pump efficiency.

Another essential parameter that needs to be established in order to improve the simulations is the temperature entering the DHN. The temperatures were once again imposed with the measured data provided by the DHN operator of Yverdon. Unfortunately, the temperatures were taken only from the 13-11-2020 to the end of July, the date on which the measurements were uploaded. Thus, the months from August to beginning of November are missing. The hypothesis was then to impose a temperature of 20°C at the exit of the STAP in order to complete the year. This temperature was chosen knowing that the temperature of the supply network has to be limited anyway to 22°C and by doing the mean between the temperatures of July and November. This constraint on the supply temperature is caused by the heat pumps that cannot be operated above 22°C. The resulting evolution of the temperature exiting the STAP is displayed in the Fig. 5.6.

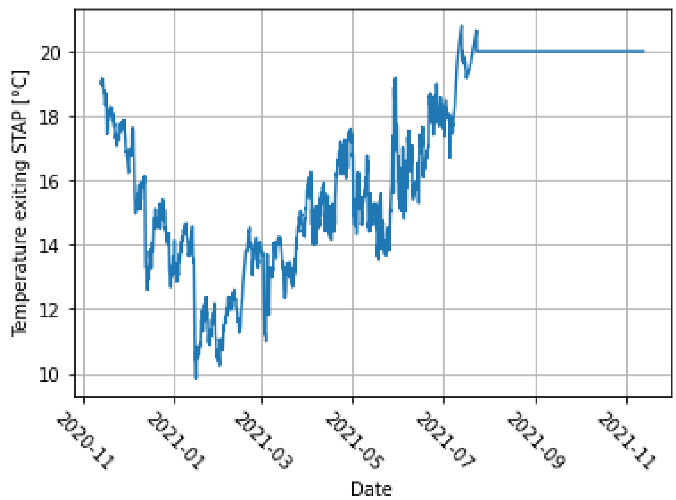


Figure 5.6: *The measured exiting temperature of the STAP with a data completion from August 2021 to the end.*

### 5.3.2 Results on the 2021 scenario

Considering all these hypotheses, simulations on the DHN of Yverdon have been carried out. In this part, no imposed heat demand was given to the input XML. The heat demanded was then computed thanks to the geometrical model built by Pierre Van Brockhoven. As for the case study of Verbier, a first validity check has been done with GIFs. This time, four indicators are used. The pressure difference is also considered since the altitude is almost constant between the different nodes. The altitude is not perturbing the pressure differences in the pipe. Only the linear and singular pressure losses are visible. The day with the higher consumption has been chosen in order to validate the robustness of the simulation and the network. The Fig. 5.7 shows the heat demand through the mass flow. In fact, the $C_p\Delta T$ is identical for all substations. As a first remark, the mass flows are approaching but not overcoming the nominal mass flow of 50 kg/s at the STAP. Looking in more detail at the simulation results, it is possible to observe that the mass flow increases at the STAP during the night from midnight to 7 am. It is quite logical since the temperatures are dropping until the sun shines in the morning. In the simulations, a comfort temperature is maintained in the buildings even though for most of them they are empty. In fact, the buildings supplied are all public facilities. Around noon, the heat supplied by the network is increasing again since people just before their break are for example going to the gym or the swimming pool and uses the showers which imply an increase in heating consumption in these types of buildings just after due to refill of the DHW tanks.

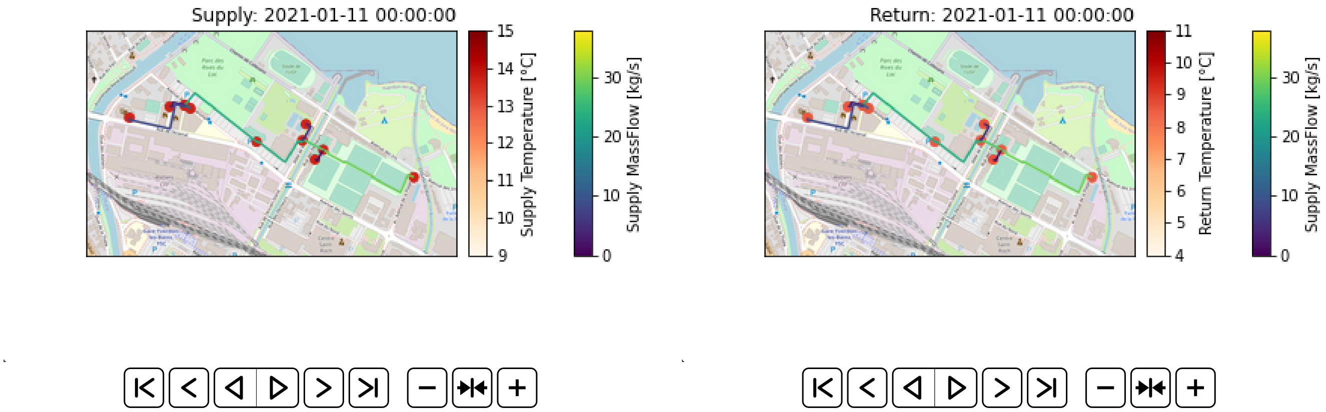


Figure 5.7: *Time evolution of the temperatures and mass flows through the actual network of Yverdon (right supply, left return). The temperatures are given at the nodes while the mass flows are given at the pipes.*

Then in the late afternoon, the after-work activities are again increasing the mass flows in the network. The mass flow then decreases slightly reaching the minimum ambient temperature at around 11 pm before rising again with the decrease of the exterior temperature until the next morning. All this shows in the end that the network is responding correctly to the heat demand.

Concerning the temperatures, they give already an insight on the thermal losses of the network. Their variation clearly shows that the thermal losses are small. The very good notice regarding the robustness of the network is that no return temperature is below the limit temperature of 4°C. Looking at the robustness of the code, the $\Delta T^{evap}_{design}$ of 5°C is respected at each evaporator.

Moving to the pressure losses in the network, they are shown in the Fig. 5.8. Only the supply pressure difference is shown as the return is very similar.

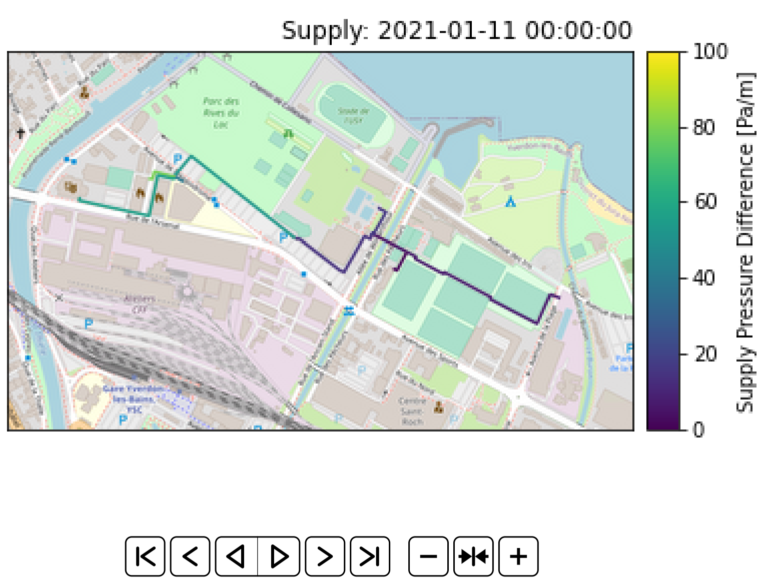


Figure 5.8: *Time evolution of the regular together with the singular pressure differences through the actual network of Yverdon.*

The linear, as well as the singular pressure losses are displayed on the GIF. It is interesting to notice that the pipe with the highest pressure differences is quite small. It is caused by the consideration of singular pressure losses. These singular pressure losses are attributed to the pipes as explained in chapter 3. Therefore, when the linear pressure difference is computed, this singular pressure difference is distributed along the pipe increasing significantly the linear pressure losses for small pipes. In the end, the plausibility check is also satisfying. The linear pressure losses are never overcoming 100 Pa/m. In the report Planair, the DN of the pipes were carefully chosen so as not to exceed 100 Pa/m. This choice was taken as a trade-off between the electricity consumed by the pump, the thermal losses, and the cost investments. Having big pipes allows reducing pressure losses inducing lower electricity consumption but increases thermal losses and the pipes with bigger nominal diameters are more expensive. These considerations will be discussed in the following paragraph.

Before showing the KPI results, the connecting heat pump needs also to be validated. This validation is made through the conservation of the energy in the system. This conservation is simply given by the equation (5.3).

$$Q_{cond} = Q_{Evap} + E_{compr} \tag{5.3}$$

Since the thermal losses at the heat exchanger are accounted in the technical efficiency, the network perfectly transfers all the power to the evaporator meaning that $\dot{Q}_{evap} = \dot{m}c_p\Delta T$. The heat pump at the Marive is studied in the Fig.5.9 on the week where the demand was the strongest.

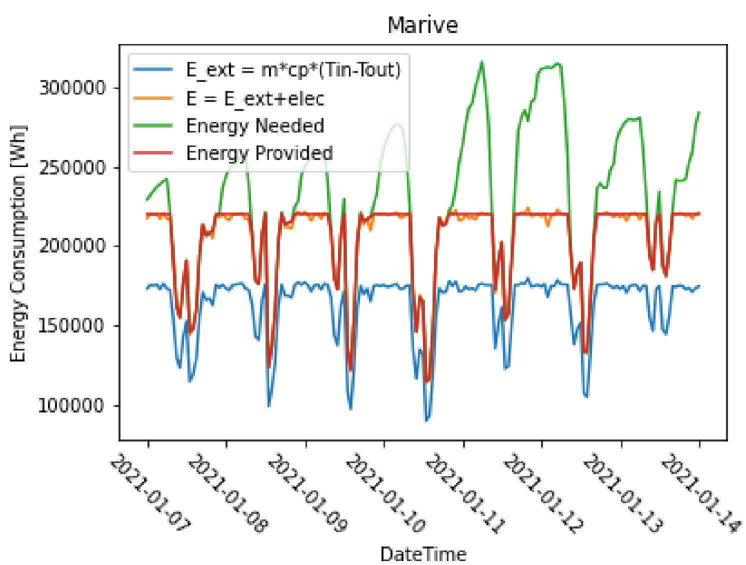


Figure 5.9: *Validation of the implementation of the SubstationHeatPump on the Marive building.*

First of all, one interesting thing to note is that the power needed by the Marive is not fulfilled. The energy needed is higher than the energy provided. The saturation comes from many factors. The first one is that the heat demand of the building is not correctly estimated even though the model is quite detailed. Once again, the buildings that are connected to the DHN are municipal facilities, which makes the estimation even harder. Indeed, the entire room inside the building might not be heated in the same way as the other or the hypothesis used for the insulation of the walls could be wrong too. Nevertheless, this saturation allows studying the energy conservation through different cases.

For the simulation, what is important is to compare the energy given by the network plus the electricity consumed by the compressor with the thermal energy that is provided to the building.

The differences occurring in the Fig.5.9 are of the order of 0.5%. These differences are simply coming from the fact that the input temperature used in the computations of $E_{ext}$ is slightly different than the one for $E$. The error is not supposed to create problems and was left unchanged.

**KPI results**

Based on all the results presented previously, the thermal losses are established and displayed in the Fig. 5.10.

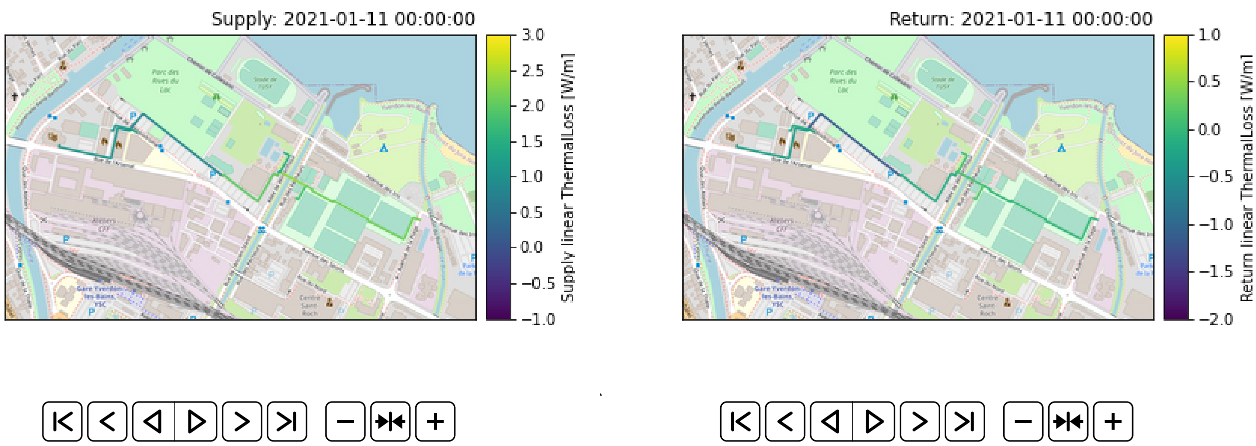


Figure 5.10: *Time evolution of the thermal losses in the actual network of Yverdon (right supply, left return).*

The thermal losses have as expected reduced in comparison to Verbier. The overall thermal losses of this network is 0.45% while the one of Verbier was about 10% of the thermal power provided by the heating station. This improvement in the thermal losses is essentially due to the reduction of the temperature between the fluid and the ground temperature. The ground temperature estimated at this day was around 6.5°C which gives a $\Delta T_{supply} \approx 8$°C and $\Delta T_{return} \approx$ 3°C. Nevertheless, it does not explain everything. Indeed, one can notice that the thermal losses are negative in the return network even though the ground temperature is smaller than the return temperature. The heating of the return pipe is coming from the pressure dissipated under the form of heat in the pipes. This effect is even more important for low temperature DHN than for hot-temperature DHN as they have generally higher mass flows through their pipes. It is corroborated with the simulation results of the Fig.5.10. The pipe in the principal network coming back from the fire station and the school and the one ahead of it demonstrates this. Their mass flows are identical as no consumers are in between but they have respectively negative and positive thermal losses. The only difference between them is their nominal diameter, see Fig.5.1. The pipe with the smaller radius has more friction than the other resulting in a higher power dissipated under the form of heat inside the pipe. Nevertheless, even though the thermal losses have decreased, reducing the size of the pipes is not a good solution since it increases the electricity consumption of the pump at the STAP. A trade-off has to be found, see the section on optimisation.

By integrating the thermal losses over the DHN, the total thermal losses are computed. On the table 5.2, the total electric consumption gathers the electric consumption of the pump with all the compressors in the heat pumps.

<table>
<tr><th></th><th>Hourly thermal losses [kWh]</th><th>Hourly electric consumption [kWh]</th></tr>
<tr><td rowspan="2">Case study 2021</td><td>2.91</td><td rowspan="2">172.9</td></tr>
<tr><td>0.45%</td></tr>
</table>

Table 5.2: *The hourly means of the thermal losses and total electric consumption in the network on the 11th of January 2021. The relative thermal losses with respect to the thermal power delivered by the wastewater treatment plant.*

In table 5.2, the means are not computed on the entire year but only on the day of interest for the validation. Interestingly, the yearly percentage of thermal losses, 1.49%, is higher than the one on the 11th of January. It is simply due to the fact that the temperatures exiting the STAP are higher in summer as shown in Fig.5.6. As the difference of temperature between the ground and the supply temperature is bigger, the thermal losses are increasing. It increases especially in the months of June and July as the ground temperature is still cold due to its inertia. This shows the importance to keep the supply temperature as low as possible in order to reduce the losses. Unfortunately, the operators do not have any controls on the temperature injected in the network as the pinch at the STAP is kept constant through the year. Nevertheless, the thermal losses are very small compared to what was observed for the case study of Verbier which highly promotes the last generation of DHN. Concerning the electricity consumption, the yearly mean is of course much smaller, only 56.4 kWh, since the heat pumps are shut down most of the summer. (Appendices put the yearly evolution of the KPIs).

## 5.4 Scenarios between the different connecting elements

In this part, different scenarios have been studied allowing to compare different connecting elements. The thermal losses and the electric consumption are once again used as KPI. The first scenario aims to compare the 1-stage heat pump with the ones with 2-stages. The second scenario shows the differences between the implementation of a centralised heat pump supplying a small district and the implementation of a personalised heat pump for each building.

### 5.4.1 Comparison between the 1-stage and 2-stages heat pumps

The two connecting elements are compared on the week of the highest consumption as for the validation of the SubstationHeatPump. The consumption of the compressors will be the highest implying bigger differences between the two cases.

A validation of the SubstationHP2stages has been performed. This validation shows very similar results to what has been done for the SubstationHP and therefore it is let in the appendices. The additional parameters used for the simulation including the 2-stages heat pump, are described in the following list of points.

- $T_{mid} = 40°C$. This temperature allows to inject the water in the secondary network at 35°C [23].
- $\eta_1 = 60\%$. This technical efficiency is taken as a 1-stage heat pump going from $T_c$ to $T_{mid}$ [22].
- $\eta_2 = 34\%$. This technical efficiency is taken as a 1-stage heat pump going from $T_{mid}$ to $T_h$ [26].

Considering these parameters, the simulations have been performed. The electric consumption of the two scenarios are compared in the Fig.5.11 and 5.12.

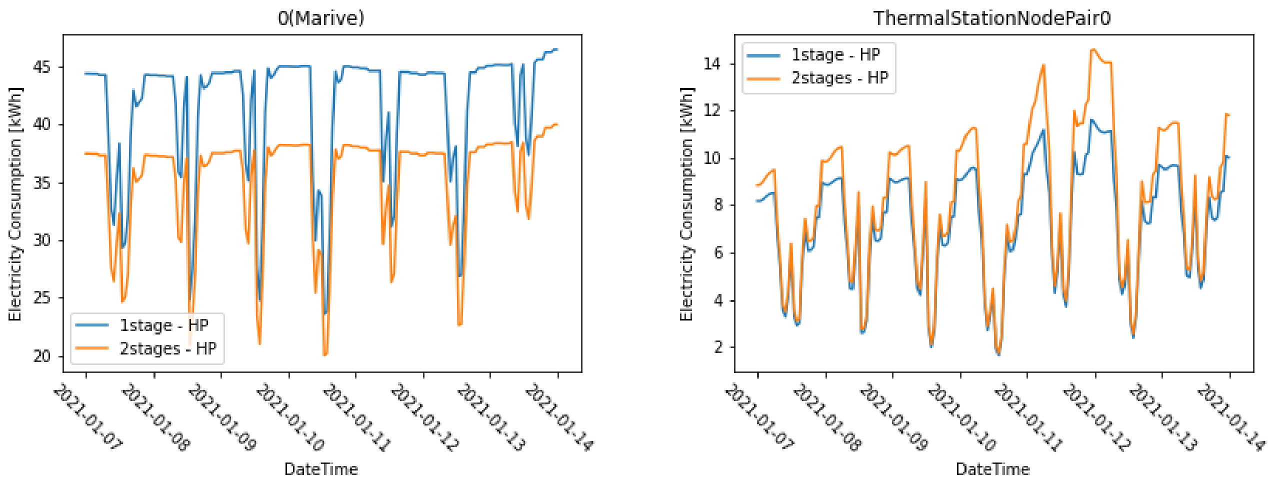


Figure 5.11: *Comparison between the electric consumption at the Marive substation (left) and at the pump of the heating station (right) with 1-stage and 2-stages heat pumps.*

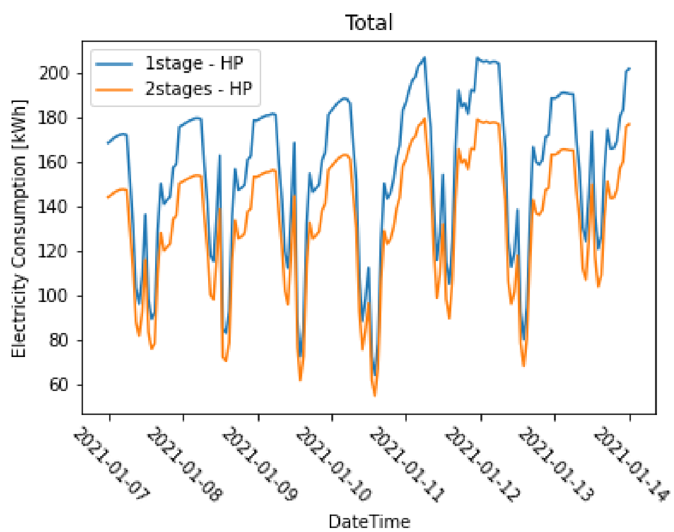


Figure 5.12: *Comparison between the total electric consumption in the actual network of Yverdon with 1-stage and 2-stages heat pumps.*

The 2-stages heat pumps allow as predicted to lower the electric consumption of the compressor as confirmed on left-hand side of the Fig.5.11. They are indeed more efficient in extracting energy from the network. It implies however to deliver a bigger mass flow to them. It results in the end in a bigger electric consumption at the heating station. Hopefully, the Fig. 5.12 shows that the network needs less electricity with 2-stages heat pumps. The use of 2-stages heat pumps during this period reduces by 14% the total electric consumption. The electric consumption goes from 26314 to 22620 kWh. A positive side effect of the implementation of the 2-stages heat pumps is the reduction of thermal losses. The thermal losses are reduced as the mass flow is increasing in the pipes. Consequently, there is more friction between the pipes and the fluid. The thermal losses decreased by 35.7% on the same period from 75684 to 48643 kWh. These differences are of course smaller considering the whole year, as the heat pumps are used less intensively on the other days. Nowadays, the multi-temperatures heat pumps are not usually implemented in district heating networks as they are more expensive on the market [22]. Hence, when considering the implementation of this kind of technology, it has to foresee the economy that is possible in its entire lifetime. For this reason, the comparison between the 1-stage heat and 2-stages heat pump is extended to the other case studies.

For the simulations of the forecast networks, the same climate file has been used as well as the same profile of exiting temperature at the STAP. The table 5.13 summarizes the results found on the different years.

| $Q_{loss}$ [MWh] | 2021 | 2022 | 2024 | 2026-Dec. |
|---|---|---|---|---|
| 1-stage HP | 30.53 | 32.76 | 32.9 | -22.2 |
| 2-stages HP | 29.82 | 32.41 | 28.8 | -26.2 |
| $\Delta_{rel.}$ [%] | 2.3 | 1.1 | 12.4 | 18 |

| $E_{cons}$ [MWh] | 2021 | 2022 | 2024 | 2026-Dec. |
|---|---|---|---|---|
| 1-stage HP | 494.2 | 546.8 | 1299 | 1861.6 |
| 2-stages HP | 410.3 | 453 | 1132.6 | 1640.6 |
| $\Delta_{rel.}$ [%] | 17 | 17.2 | 12.8 | 11.8 |

Figure 5.13: *Annual KPIs for the different forecast extension of the network*

The table shows the thermal losses and total electric consumption in one year. The results of the last case study could be surprising since the thermal losses are negative. In the last case, the mass flows are reaching the hundreds of kg/s, and therefore higher frictions are occurring in comparison to the other cases. The total electric consumption demonstrates that more demand is asked from the network.

The results obtained with the simulations are quite promising for the multi-temperature heat pumps. Nevertheless, non-negligible parameters have not been taken into account. The first one is the price of this type of technology. As previously mentioned, they are more expensive due to their complexity. As it is more complex, it requires also higher maintenance costs. In the end, this analysis is done for one particular case but it shows what CitySim is capable of.

### 5.4.2 Comparison between centralised and decentralised heat pumps

When building a low temperature district heating, one has the choice to use centralised heat pumps with smaller secondary high temperature district heating or having multiple individual heat pumps for each building. The centralised heat pumps allow to have bigger and therefore custom installations that are generally more efficient. The total power installed could also be reduced since the peak of demand might not be at the same time if different types of buildings are supplied by the centralised heat pump. In the case of Yverdon, the installed centralised power is, unfortunately, higher than the sum of the decentralised as there are more thermal losses. In addition, the buildings connected to the network are almost all of the same type. Connecting buildings of the same type does not allow to reduce the power installed since they have similar profiles of heat demand and therefore the demand is not well distributed during the day.

The interest is also coming from the fact that grants are given for the development of high temperature district heating. According to the Canton de Vaud, a district heating network starts at five buildings connected [9]. For many operators of district heating networks, the help of the confederation is essential as the investments requested for the development of this technology are usually given in millions of CHF. In the specific case of Yverdon, this grant could be very useful for financing future extensions.

On the other hand, the decentralised heat pumps allow having low temperatures until the consumer reducing the thermal losses. It permits also to have only one district heating network and therefore a simpler system.

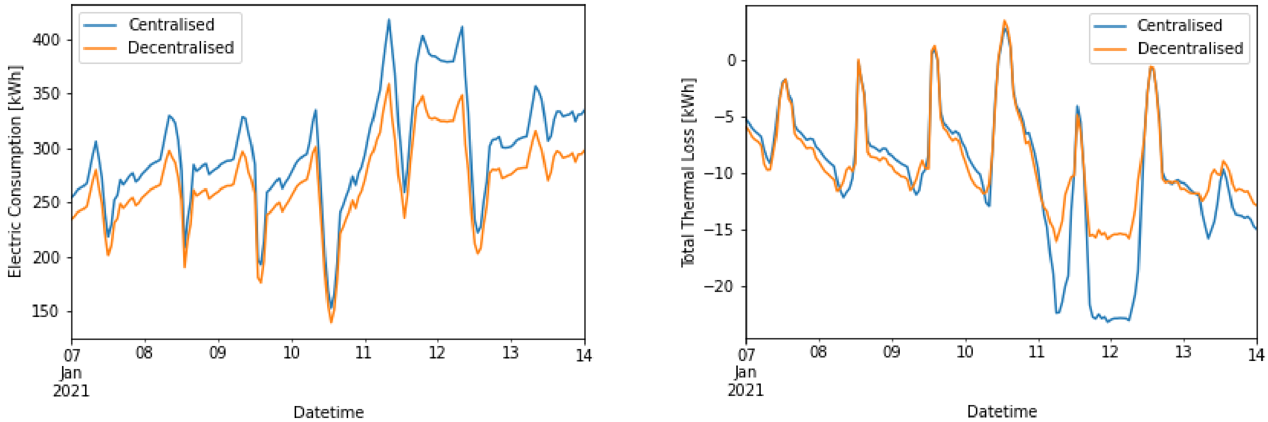


Figure 5.15: *Comparison between the decentralised and centralised heat pump cases on the electricity consumption (left) and thermal losses (right) on the low temperature DHN.*

For this comparison, the case study of 2026 has been considered. The difference between the centralised and decentralised is shown in the Fig. 5.14. The centralised heat pump is supplying more than five buildings in order to have a high temperature district heating network in the second hand.

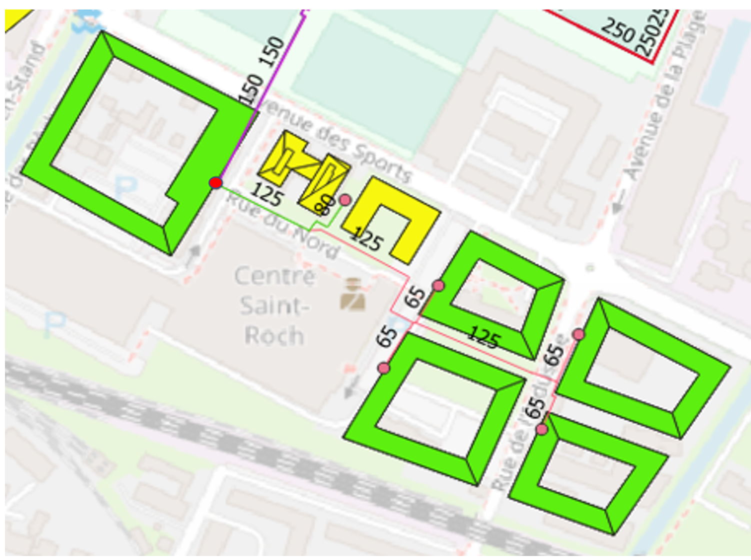


Figure 5.14: *QGIS visualisation of the centralised heat pump and the decentralised heat pump scenarios. The centralised heat pump is represented with the red point and supplies all the buildings on the map.*

For the centralised heat pump scenario, the secondary high temperature district heating has not been modeled. The heat demand of all the buildings connected to the high district heating network has been previously established and a thermal loss of 10% has been assumed. The resulting total heat demand has then been imposed to the centralised heat pump.

Considering these hypothesis, the different scenarios have been simulated. The results of the comparison are displayed in the Fig.5.15. The Fig.5.15 shows that the centralised heat pump consumes more electricity than its decentralised counterpart. More electricity is consumed as the centralised heat pump has to provide more energy to the eco-district in order to compensate additional losses of the high temperature district heating network. Moreover, it implies increasing the mass flow in the network. The pump at the STAP is then also consuming more electricity. The difference is even increasing on the 11th of January as the mass flow reaches 120 kg/s at the exit of the pumps. As previously stated in the discussion of the table 5.13, the pressure losses have a square dependency with the mass flow. The pump needs to compensate these pressure losses in order to provide for the needs of every consumer increasing again its electricity consumption. A solution to this problem would be to increase the radius of the pipes. The GIF 5.16 displaying the pressure difference in the network with the centralised heat pump shows that especially the pipe connecting the eco-district heat pump to the principal network is generating big pressure differences. Looking at the pressure difference in the previous pipe on the principal network with DN 250 demonstrates the improvement that is possible with an increase of the pipe size.

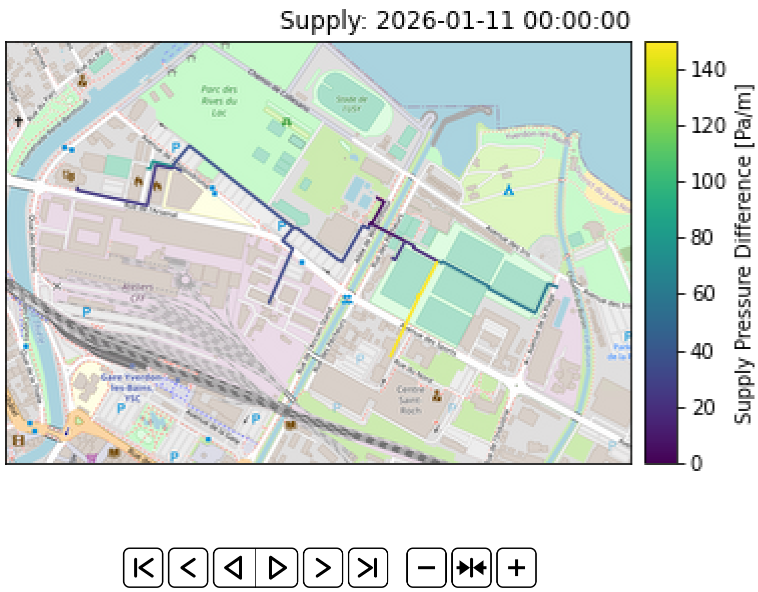


Figure 5.16: *Time evolution of the pressure differences through the forecast centralised network of 2026 in Yverdon.*

Going from a DN 150 to a DN 250 could reduce the pressure losses of a factor 2 which will result in lower electricity consumption for the pump, especially for the centralised case.

Friction allows on the other hand to gain more heat and to reduce the thermal losses. However, the gain in thermal losses for the centralised case is not significant, even though more frictions occur in the pipes. The eco-district represents 23% of the heat demand of the network. Adding 10% of thermal losses increases the heat delivered by the DHN increasing at the same time the absolute thermal losses which competes with the heat gains through frictions.

The yearly results of the comparison are summarized in the table 5.3.

| | Centralised [MWh] | Decentralised [MWh] | $\Delta_{rel.}$ [%] |
|---|---|---|---|
| Electricity consumption | 983.9 | 893.4 | 9.2 |
| Thermal losses | -20.5 | -22.2 | -7.7 |

Table 5.3: *Comparison of the yearly KPIs between the centralised and decentralised heat pump.*

In the end, the decentralised case seems to be more profitable for both KPIs when the whole year is considered. For the centralised case, the additional thermal losses due to higher energy provided by the DHN overcome the additional heat gains due to pressure dissipation. As seen in Fig.5.15, the thermal losses were lower than in the decentralised case only when the electric consumption (i.e. mass flow) was above a certain threshold. Nevertheless, many other factors are coming in when considering the two scenarios. As an example, the comparison between centralised and decentralised heat pumps was considered without any solar thermal power injections in the DHN. However, as it is addressed in the following section, the temperature of the district heating network is a key parameter on the efficiency of the solar thermal injection. The KPIs give good guesses of what is the best but in the end, when a trade-off has to be made, it depends on each DHN. For example in the case of Yverdon, the thermal losses might not be crucial as the electricity consumption since the heat is coming from the wastewater treatment plant which is, of course, limited but given for free.

## 5.5 Solar district heating

This part aims to evaluate the injection of solar thermal in low temperature district heating networks. Hence, contrasting with the previous scenarios, the buildings are now capable of injecting their heat excess inside the network. In the recent years, many case studies of solar district heating have appeared, especially in the Nordic countries such as Denmark. It is needed to inject the solar thermal at the same temperature as the one from the heating station in order to not impact negatively other consumers. The pressure difference around the pump of the prosumer is assumed to be equal to the one at the heating station. This prevents one of them from taking the lead of the other. The latter, which is in producer mode, would then have the flow going in the wrong direction through its pump.

### 5.5.1 Comparison between centralised and decentralised injection

A question that is usually asked when implementing solar panels in a district heating network is whether to run a centralised installation of solar thermal panels or to distribute the panels on the roofs of the different consumer. In the first case, the network is easier to manage. There is only one prosumer that injects the heat. The problem is that it needs a lot of space in order to install every solar panel. Therefore, it is not suitable to implement this solution in cities where the district heating network is particularly interesting. In the second case, the decentralised installation uses free spaces on the roof of the consumers. Thus, they can directly supply the consumer or inject into the network. The drawback is that it is more complex to deal with, since many different consumers can become all at once producers, reversing the flows in the pipes as they usually inject in the supply pipe.

In this section, the performance of both solutions in the network is investigated. To do so, the same surface of solar thermal panels has been considered. In the decentralised case, the panels are distributed on every roof top of the new coming buildings, as forecasted by the municipality of Yverdon. In the centralised case, it has been decided to virtually locate all these panels at the *ILOT_4* visible in the Fig.5.1. Combining all the panels of the roof tops give an overall area of 20497 m$^2$ according to CitySim. The results are given in the table 5.4.

The results from the table 5.4 show that the heating station consumes less for centralised case. This means that the centralised case is more efficient in supplying its consumer counterparts than the decentralised one. It is explained by the fact that in a low temperature district heating network, the temperature is lower in the network than the one in the building. Consequently, according to the formula of the efficiency of the solar thermal panels, the panels are thus more efficient at heating the network than themselves.

| | $Q_{deliv.}$ [MWh] | Electricity consumption [MWh] | Thermal losses [MWh] |
|---|---|---|---|
| Centralised | 7265 | 2324.0 | -45.4 |
| Decentralised | 7456 | 2356.2 | -55.16 |
| $\Delta_{rel.}$ [%] | -2.6 | -1.4 | -2.1 |

Table 5.4: *The comparison of the total thermal power provided by the heating station, total electricity consumption and total thermal loss between the centralised and decentralised solar injection over one year.*

### 5.5.2 Sizing of the storage heat tank

The problem of solar thermal injection as well as for every renewable energy is that it is intermittent. In fact, solar thermal will produce more energy during the summer when the heat demand lower and the production is low in winter when the heat demand is high. Therefore, in order to have some interest in implementing solar thermal, it needs to be coupled to a seasonal storage system. The seasonal storage permits to redistribute into the network, the excessive heat provided by the solar panels in summer, during the cold days in winter. In the case of Yverdon, it is even more interesting because of the range of operation of the heat pump. As the network is connected to a WWTP, they do not have control over the supply temperature. This is already causing some issues for the heat pumps since they have to be operated under a certain threshold. The seasonal storage, if it is designed big enough, can be used also as a conditioner for the network. In the case of this work, a simple optimization of the sizing of the storage tank is carried out. Indeed, these tanks have to store a lot of energy which translates into huge volumes that are usually placed at the heating station. In the case of a low temperature district heating network, this problem of sizing is even bigger since the difference of temperature is only of 5°C. In the Fig.5.17, different heat capacities have been compared by considering a constant injected temperature of 12°C.

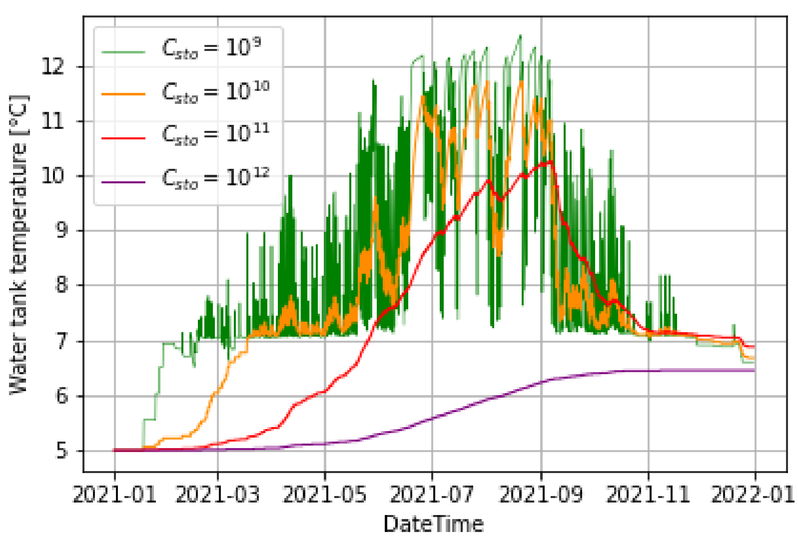


Figure 5.17: *Evolution of the temperature inside the storage tank at the heating station for various heat capacity in J/K for the first year of operation.*

The different behavior of the tanks can be explained as such. Concerning the smaller heat tank, its temperature is increasing much faster since it needs less energy to be heated up. Therefore, it is the fastest one to help the energy conversion unit and in this case the WWTP. As it is smaller, it is discharged more rapidly than the others which creates these oscillations. The smaller heat capacity is probably not the best choice since it usually hits the lower limit, which means it was empty even though the boiler still required some energy. These oscillations are reduced by increasing the capacity of the storage tank since an equivalent drop in temperature of the water tank delivers 10 times more energy than its lower size counterpart. In the end, for the biggest capacity at $10^{14}$J/K, it does not even succeed to reach the entering temperature. Therefore, it is never discharged in the first year of operation meaning that it is probably not the most appropriate size of tank neither.

The optimal size of the tank is the one allowing the smallest heat delivered by the WWTP. The table 5.5 displays the total heat delivered by the heating station through the year 2021.

| $C_{sto.}$ [J/K] | $10^9$ | $10^{10}$ | $10^{11}$ | $10^{12}$ |
|---|---|---|---|---|
| $Q_{deliv.}$ [MWh] | 7515.78 | 7475.3 | 7456.3 | 7631.4 |

Table 5.5: *The energy delivered by the WWTP during the year 2021 considering different sizes of storage.*

Looking at the table 5.5, the storage capacity of $10^{11}$J/K has been identified as the best candidate. Given the capacity of the storage system, it corresponds already to a volume of 24'000 m$^3$ which is the equivalent of ten Olympic swimming pools. Regarding the KPIs of the electricity consumption and the thermal losses, they are not used for the evaluation of the best candidate. These quantities are independent of the size of the storage since the heating station still injects at 12°C in the supply network and the heat demand of the building is not perturbed by the installation. Therefore, the heat pumps delivering the heat to the consumers will have the same efficiency and same power to deliver.

For a more complete study, it could also have been interesting to look at the evolution of the temperature in the following years as the input temperature of every storage system is higher at the end of a year than at the beginning. It could become then profitable to invest in an even larger storage system as this technology is supposed to last for decades. Considering the following years is hence mandatory if a more precise sizing of the tank is desired. Additionally, in further development of the tool CitySim, it could be interesting to implement other kind of seasonal storage as many of them exist using different processes such as phase change or chemical processes [27].

### 5.5.3 Comparison between different injection temperature

In this section, another interesting parameter to vary is the injection temperature of the solar thermal and the heating station, since the performance of many elements is depending on it. On one hand, the efficiency of the panels evolves with the temperature, following the equation (2.2). When the $T_{inj.}$ is decreasing, the efficiency of the panels increases as less heat is dissipated to the environment. On the other hand, the thermal losses are decreasing with the injection temperature. Similarly, the efficiency of the heat pump is also decreasing with the injection temperature. In the end, the change of heat delivered by the heating station is a summation of all these effects. The heat pump increases $Q_{deliv.}$ with the temperature decrease, while the other two parameters have the opposite effects.

For this study, the usual decentralised case is considered with a seasonal storage system of $10^{11}$J/K. The table 5.6 summarizes the results for the different injection temperatures evaluated. For the temperatures, they are assumed constant through the year for simplicity. It has been chosen to stay in the range between 10°C and 20°C since, for the upper limit, the heat pump does not like to be operated above it. Regarding, the lower limit, it is respecting the recommendation of the Planair report as it is not desired to go below 4°C in the return network. As the design temperature difference is set at 5°C, a margin of one degree has been kept by considering this lower limit of injection at 10°C.

| $T_{inj.}$ [°C] | 10 | 12 | 14 | 16 | 20 |
|---|---|---|---|---|---|
| $Q_{deliv.}$ [MWh] | 7331.9 | 7475.3 | 7566.4 | 7684.1 | 7918.9 |
| Electric Consumption [MWh] | 2432.2 | 2343.5 | 2303.7 | 2219.7 | 2053.9 |
| Thermal Losses [MWh] | -71.4 | -54.0 | -38.2 | -20.5 | 13.6 |

Table 5.6: *The energy delivered by the WWTP along the KPIs considering different temperatures of injection.*

Following the table 5.6, a trade-off has to be made as predicted by the different effects that are taking place. In the case study of Yverdon, this trade-off is simpler since the heat delivered is given for free. Interestingly, in this very specific case, it might be profitable to increase the temperature of the network which is totally counterintuitive with respect to the storyline of the district heating network. Of course, this should be done carefully as the heat delivered by the WWTP is limited or could be used for other purposes. Hence, it should not be wasted.

# CHAPTER 6

# CONCLUSION

In conclusion, this thesis inserts itself in a context where our modern societies are based on energy consumption. In the incoming years, this would become an issue since most of the energy consumed is supplied by fossil fuels. Since they are non-renewable, there is an urgent need to find alternative means in order to produce energy. Nowadays, some renewable energies are existing such as solar thermal panels or windmills. Nevertheless, these technologies are intermittent since they always depend on weather condition, which slows down the penetration of these technologies in the current energy mix.

In order to facilitate their integration, the district heating network is considered one of the most promising technology. Hence, the implementation of district heating networks has accelerated in the past years. Therefore, software such as CitySim are required in order to simulate and dimension correctly the new installation.

This thesis tried to validate and further improve CitySim. The implementations of the singular pressure losses and especially of the MCR participate in this improvement of the simulation. CitySim was then tested with the case studies of Broc and Verbier. Comparing the simulation results with the measurements acquired from the operators of both district heating networks allowed to validate this tool.

Then, CitySim has been applied to the low temperature district heating network case study of Yverdon. In order to achieve this, the 1-stage and 2-stages heat pumps have been implemented and validated. From there, scenarios of different connecting elements have been simulated. The results have shown, in the case of the comparison between the 1-stage and the 2-stages heat pumps, the possible improvements due to implementation of two stages heat pumps. Similarly, the centralised and decentralised heat pumps have also been compared. The results show that the decentralised case was favoured in terms of electricity consumption and thermal losses. Nevertheless, these results should be considered in a bigger picture since external elements could influence the decision. As an example, even though the decentralised case more efficient, the centralised case could have been more profitable due to grants that are given to high temperature district heating networks.

As a last study, CitySim has been used in order to simulate three different scenarios of solar injections in the 2026 forecast network of Yverdon. These scenarios pointed out in the end the advantages of combining solar thermal with low temperature district heating and evaluate the different operating conditions of solar and seasonal heating in order to get the best performance from it. This type of evaluation is essential in order to promote these technologies to the people.

In the end, CitySim can be of a great help in decision-making. Therefore, it has to be further improved by implementing new algorithms or new devices in order to converge faster and give more information to the politics that can make the difference.

# Bibliography


[1] Hannah Ritchie and Max Roser, *Energy*, Our World in Data, (2020), https://ourworldindata.org/fossil-fuels, Accessed: 2021-08-02

[2] Word Health Organization, *Ambient air pollution attributable deaths*, https://www.who.int/data/gho/data/indicators/indicator-details/GHO/ambient-air-pollution-attributable-deaths Accessed: 2021-08-02

[3] Swiss Federal Office of Energy, Bafu, *What is the Energy Strategy 2050?*, https://www.bfe.admin.ch/bfe/en/home/policy/energy-strategy-2050/what-is-the-energy-strategy-2050.html, Accessed 2021-08-02.

[4] Swiss Federal Office for the Environment, Bafu, *Switzerland's greenhouse gas inventory*, https://www.bafu.admin.ch/bafu/en/home/topics/climate/state/data/greenhouse-gas-inventory.html, Accessed 2021-08-02.

[5] Project drawdown, *Solutions 101*, https://www.drawdown.org/climate-solutions-101, Accessed 2021-08-02

[6] Swiss energy, OFEN, *Energy field* https://www.bfs.admin.ch/bfs/en/home/statistics/construction-housing/buildings/energy-field.html, Accessed 2021-08-02

[7] HögforsGST, *Future of District Heating* (19/05/2020),https://www.hogforsgst.com/news/future-district-heating-part-1-past#, Accessed: 2021-08-02.

[8] Swiss energy, OFEN, *Handbook on Planning of District Heating Networks*, (09.2018)

[9] Etat de Vaud, Official website, *17. Demander une subvention pour une nouvelle construction ou extension du réseau de chaleur (CAD); nouvelle construction ou extension de l'installation de production de chaleur*, https://www.vd.ch/prestation-detail/prestation/15-demander-une-subvention-pour-une-nouvelle-construction-ou-extension-du-reseau-de-ch Accessed 2021-08-02.

[10] Dan Wang, *et al.*, *Optimal scheduling strategy of district integrated heat and power system with wind power and multiple energy stations considering thermal inertia of buildings under different heating regulation modes, Applied Energy*, **240**, p. 341-358, (2019), ISSN 0306-2619, https://doi.org/10.1016/j.apenergy.2019.01.199.

[11] Karl Martin Heissler, *et al.*, *Modeling low temperature district heating networks for the utilization of local energy potentials*, Bauphysik, **200**, (2016), DOI:10.1002/bapi.201610038

[12] Dominik Hering, Mehmet Ege Cansev, Eugenio Tamassia, André Xhonneux, Dirk Müller, *Temperature control of a low-temperature district heating network with Model Predictive Control and Mixed-Integer Quadratically Constrained Programming*, Energy, **224**, 2021, 120140, ISSN 0360-5442, https://doi.org/10.1016/j.energy.2021.120140.

[13] P. Monsalvete Álvarez de Uribarri, Ursula Eicker, Darren Robinson, *Energy performance of decentralized solar thermal feed-in to district heating networks*, Energy Procedia, **116**, (2017), Pages 285-296, ISSN 1876-6102, https://doi.org/10.1016/j.egypro.2017.05.075.

[14] Pierre Cognet, *DISTRICT ENERGY NETWORK SIMULATION FOR THE EVALUATION OF SOLAR THERMAL POTENTIAL*, (08.2020), Master thesis

[15] Ziying Liu, Tianlai Yu, Ning Yan, Lipeng Gu, *Variation of Ground Temperature along the Stratum Depth in Ice-rich Tundra*, Geosciences 2020, 10, 104, (07.2020) https://doi.org/10.20944/preprints202002.0095.v1

[16] Linn Saarinen, *Modelling and control of a district heating network*, (03.2008), http://www.diva-portal.se/smash/get/diva2:461661/FULLTEXT01.pdf

[17] EPFL Website on CitySim software, EPFL, *CitySim software*, https://www.epfl.ch/labs/leso/transfer/software/citysim/, Accessed 2021-08-15

[18] Dr. J.-P. Corbat, Ph. de Werra, *3.Dynamique des fluides non compressibles*, EIA, (1969)

[19] Thomas Oppelt, *Modell zur Auslegung und Betriebsoptimierung von Nah- und Fernkälstenetzen*, (10.2015), PhD thesis

[20] QGIS Development Team. QGIS Geographic Information System. Open Source Geospastial Foundation. 2009. URL: http://qgis.osgeo.org.

[21] Pierre Van Brockhoven, *Solar Thermal energy in a district heating system: A case study analysis*, (06.2021)

[22] Cordin Arpagaus, *et al.*, *Multi-temperature heat pumps: A literature review*, International Journal of Refrigeration, **69**, p.437-465, (2016), https://doi.org/10.1016/j.ijrefrig.2016.05.014

[23] Brian Elmegaard, *et al.*, *Integration of space heating and hot water supply in low temperature district heating*, Energy and Buildings, **124**, p.255-264, (2016), https://doi.org/10.1016/j.enbuild.2015.09.003

[24] PLANAIR SA, *CAD STEP, Yverdon-les-bains*, (12.2018)

[25] Brugg, *Premant datasheet*, (06.2019)

[26] Mitsubishi electric, Hydronics and IT cooling systems, *Climaveneta data sheet*, (2016)

[27] Kai Nielsen, *Thermal Energy Storage - A State of the Art*, a report within the research program Smart Energy-Efficient Buildings at NTNU and SINTEF 2002-2006, 2003